Journal of Energy Storage 65 (2023) 107299

Contents lists available at ScienceDirect

Journal of Energy Storage

journal homepage: www.elsevier.com/locate/est

Research papers

Efficiency characterization of 26 residential photovoltaic battery storage systems

Nico Orth [a,*], Nina Munzke [b], Johannes Weniger [a], Christian Messner [c], Robert Schreier [b], Michael Mast [b], Lucas Meissner [a], Volker Quaschning [a]

[a] HTW Berlin – University of Applied Sciences, Department 1 – Energy and Information, Wilhelminenhofstraße 75 A, D-12459 Berlin, Germany
[b] Karlsruhe Institute of Technology (KIT), D-76344 Eggenstein-Leopoldshafen, Germany
[c] Austrian Institute of Technology (AIT), A-1210 Wien, Austria

ARTICLE INFO

Keywords:
Electric energy storage
Photovoltaic battery system
System losses
Performance
System comparison
Efficiency

ABSTRACT

Numerous loss mechanisms contribute to the overall performance of stationary battery storage systems. From an economic and ecological point of view, these systems should be highly efficient. This paper presents the performance characteristics of 26 commercially available residential photovoltaic (PV) battery systems derived from laboratory tests. They were measured according to the efficiency guideline for PV storage systems. Nine AC-coupled and 17 DC-coupled lithium-ion battery systems are compared. Their measured usable energy content varies between 5.8 kWh and 16.7 kWh and is in some cases more than 19 % below the specifications in the data sheets. Besides the usable capacity, the nominal power and the efficiency of the power conversion system are analyzed. DC-coupled PV storage systems are often advertised with inherently higher efficiency compared to AC-coupled systems. However, the comparison shows that they depend on high battery voltages of several hundred volts in order to exploit their efficiency advantages. The most efficient systems achieve average conversion path efficiencies of more than 97 %. In contrast, the values of the least efficient systems evaluated are only 90 %. Furthermore, the paper analyzes the control behavior by comparing the dead and settling times as well as the stationary control deviations of the investigated systems. Differences in the dead time of almost 3 s and in the settling time of more than 13 s can be observed. In addition, the AC, DC and peripheral power consumption in the fully charged and discharged state are evaluated. While individual systems have an outstanding power consumption of less than 4 W in the standby mode, others consume more than 70 W. The paper shows that various systems still have potential for optimization, especially in terms of conversion efficiency and standby losses. When selecting or optimizing a PV battery system, it is important to consider all loss categories to achieve high overall efficiency.

1. Introduction

The transition to a decarbonized and clean energy system is crucial given the dependence on fossil fuels and the devastating consequences of climate change. Energy storage is a key to overcoming the variability and volatility of renewable energy sources [1]. Especially battery storage systems are frequently addressed as the technology that may unlock this transition [2,3]. Over the last few years, a strong increase in the number of installed battery systems can be identified. In 2017, the International Renewable Energy Agency (IRENA) reported a worldwide installed capacity of stationary battery systems of just under 11 GWh [4]. From 2018 to 2020, large-scale battery systems with an energy capacity ranging from 0.2 MWh to 250 MWh and a total capacity of around 1.5 GWh were installed in the U.S. [5]. In contrast, during the same period about 2.3 GWh have been added in the residential sector in Europe alone [6]. The same study also shows that Germany accounts for around 70 % of the total European home storage market. According to Jo et al., the residential market is also booming in Korea. In 2018 alone, domestic storage systems with a cumulative capacity of about 1.5 GWh were installed [7]. Globally, an additional 25 GWh of stationary storage has been installed between 2018 and 2020 [8]. The analysis of BloombergNEF also shows that the number of utility-scale systems predominates, but there has been a continuous increase in residential storage. Of the storage systems installed worldwide in 2020, with a

* Corresponding author.
E-mail address: storage-systems@htw-berlin.de (N. Orth).

https://doi.org/10.1016/j.est.2023.107299
Received 29 December 2022; Received in revised form 24 March 2023; Accepted 28 March 2023

cumulative capacity of 11 GWh, the residential sector accounts for around 25 % [8]. Lithium-ion batteries have become the dominant technology for battery storage systems [8–10]. At the same time, as manufacturing capacity increases and technological innovations continue, their costs are constantly declining [2,11].

1.1. Home storage market in Germany

Germany is one of the pioneer markets for the development of stationary battery systems worldwide [9], especially in the residential sector [12]. Using photovoltaic (PV) combined with a battery system is considered a key technology for more ecological sustainability in the residential sector [13]. The solar potential on German buildings is considerable. Mainzer et al. indicated a potential for roof top PV systems on residential buildings of more than 200 GW [14]. Like other countries around the world, Germany introduced subsidy programs that successfully incentivized investment in residential PV systems [15]. In 2021, more than 215,000 PV systems up to 30 kW were installed in Germany [12]. By the end of the year 2021, there were more than 2 million PV systems in this market segment with an installed capacity of 20.4 GW [16]. This corresponds to a share of one third of the total solar capacity installed in Germany [17].

Since 2012, electricity prices for households have exceeded feed-in tariffs [9]. In conjunction with the decreasing costs for PV and battery systems as well as the falling grid feed-in tariff, it has become increasingly economical to raise the level of self-consumption in recent years [18]. According to Figgener et al. over 60 % of the 215,000 newly registered PV systems were installed in combination with a home storage system. If retrofits are taken into account, the total number of installed battery systems for 2021 reaches about 145,000 [12]. Other estimates from the German Solar Association (BSW) (141,000) and EUPD Research (135,000 to 150,000) are in a similar range [17,19,20]. Overall, the market is assuming a stock of 430,000 home storage systems with an installed capacity of 3.5 GWh in Germany by the end of 2021 [12]. Within just a few years, PV home storage systems in Germany have developed from a niche product into a large market with more than 60 manufacturers and suppliers with several hundred different system combinations up to 30 kWh [21]. The available systems have a wide range of different characteristics. For example, systems with different topology (AC- or DC-coupled) and technology (lithium-ion or sodium-nickel chloride) are offered. Furthermore, the systems differ in terms of power capacity and energy content (in the following battery capacity) as well as battery voltage level (low or high voltage). In addition, the connection of the storage system to the power grid (single- or three-phase) can be different.

1.2. The relevance of system efficiency

The main objective of a PV battery system for the power supply of residential buildings is to reduce the power drawn from the grid as much as possible. However, by storing the excess PV power, the energy fed into the grid is reduced. When operating a PV battery system, it is therefore desirable due to economic reasons to minimize the amount of power drawn from the grid as much as possible while achieving the highest possible PV feed-in [22]. Accordingly, the amount of system losses that have an impact on the energy exchange with the grid is crucial [23]. The different losses can be separated into four main categories: sizing, conversion, control, and standby-related losses [24,25]. The sizing losses occur due to the power dimensioning of the system components, which result from the limitation of the power electronics. The energy conversion in the battery system and in the power electronics is subject to further losses. In addition, there are control losses, which are mainly caused by the delayed and inaccurate power consumption and output of the battery system. The power consumption of the components in the fully charged or discharged state results in so-called standby losses. In addition, energy management-related losses can occur. For grid-serving reasons, a limitation of the grid feed-in power to e.g. 70 % of the nominal power of the PV generator can be required in subsidy programs. If the excess power is not stored, the power output of the PV generator must be curtailed by no longer operating the PV generator at the maximum power point (MPP). The curtailment is associated with a decrease in the energy output of the PV system. According to different sources, the performance of a PV battery system also includes system reliability and aging effects [26–29].

The study by Munzke et al., for example, demonstrates that system losses can be significant. The results show that even in a comparatively small-sized PV battery system with a nominal power of 3.5 kW and a usable battery capacity of 4.4 kWh, total losses of up to 950 kWh/a can occur [23]. In this case, the losses can especially be attributed to the power conversion and the MPP tracking. In contrast, the total losses of a high-efficient 12.2 kWh battery system combined with a 10 kW PV system are less than half as high (405 kWh/a), although energy throughput increases with the system size [30]. In addition, it should be noted that the overall system efficiency, charging strategy and the aging of the battery and PV system might also have a significant impact on the sizing of PV battery systems and thus on the investment costs [31–33]. At the same time, simulation analyses show that system efficiency can have a greater impact on the degree of self-sufficiency than the usable battery capacity [34].

In addition to economic considerations, battery systems should also operate highly efficiently for environmental reasons. To ensure that the use of storage systems only has a small impact on the environmental relief achieved by the PV system, low storage losses are crucial [35]. The higher the energy efficiency of the battery systems, the lower the carbon dioxide, sulfur dioxide and nitrogen oxide emissions from the fossil-fuel power plants that results from the remaining grid supply, especially during winter [36].

For the reasons mentioned above, among others, the efficiency of a storage system is one of the 5 most important selection criteria for installers, along with quality issues and warranty conditions [37]. For the end customers, hedging against rising electricity prices and their own contribution to the energy transition are usually the decisive factors for the purchase of a PV battery system [38].

1.3. Methods for characterizing efficiency

Data sheets are intended to facilitate product selection by summarizing the most important technical characteristics of a PV battery system. However, a comparison of the data sheets reveals that the level of detail of the information and the test conditions vary considerably in some cases. Comparable performance indicators can currently only be found in a few data sheets [34]. This makes it particularly difficult for non-specialists to compare and find efficient PV battery systems. Another challenge for comparability is the degree of integration of the systems [39]. In addition, to complete systems containing all components of a PV storage system, individual components (e.g. the battery storage or the battery inverter) are also offered. Uniform procedures and metrics determined by independent testing institutes can help to objectively compare the performance and functions of various products and systems [40]. Standard test protocols may also help to perform an assessment and subsequently improve the design of storage systems regarding efficiency, battery aging, reliability, and cost [41]. Moreover, customers can be assured that the evaluated products that go through this process will meet the performance required for their applications [42].

Different methods for analyzing the energy efficiency of PV battery systems have been part of numerous research activities in the past, e.g. [22,23,43–48]. A simplified distinction can be made between field, application, laboratory and simulation testing [23]. The advantages and disadvantages of these four test specifications have already been discussed in detail [22–24,45].

The focus of this work is on the comparison of numerous

performance-related characteristics that have been determined in detailed laboratory tests. In general, these tests aim to measure individual efficiency characteristics under uniform conditions. The goal is to provide specific, repeatable and detailed test procedures. However, there are various approaches to test battery systems, as well as different examination objectives and depth of detail depending on the test directive. When conducting tests, battery cells and individual components, battery modules or the entire system can be tested.

For example, Mulder et al. developed detailed test methods for improved battery cell understanding with a focus on battery performance, aging effects and safety aspects [49]. Furthermore, according to the international standard IEC 61427-2:2015 performance characteristics like the battery capacity and round-trip efficiency (RTE) of battery systems can be evaluated in a seven-day endurance test [50]. However, the test sequence requires that the battery discharge power is at least 3 kW. This guideline is essentially battery chemistry neutral and covers different application scenarios like frequency regulation or PV energy storage time-shift. However, power conversion systems and components as well as associated interfaces are not covered by this standard, as it focuses primarily on the battery itself.

Testing the whole system is beneficial because it gives the best picture of how the system will respond. Unfortunately, this process is more expensive and usually the entire system must be installed to conduct these tests [51]. The probably best-known test guideline for energy storage systems is 'The Protocol for Uniformly Measuring and Expressing the Performance of Energy Storage Systems' prepared by the Pacific Northwest National Laboratory (PNNL) and Sandia National Laboratories [52]. The Protocol contains procedures for administering reference performance tests on energy storage systems to derive capacity, efficiency, responsiveness, standby losses and self-discharge rate. Additionally, application-specific duty-cycle performance tests are provided for a number of grid services including e.g. frequency regulation, peak shaving and PV smoothing. The energy storage system is considered a black box with power exchange between the energy storage system and the grid being measured [53]. However, usually the test procedure is applied to bigger storage systems [54,55] with the ability to supply specific services to electric grids [56,57]. The performance protocol was directly incorporated into a Standard of the National Electrical Manufacturers Association (NEMA) published in 2019 [58]. Additionally, parts of it are included in the IEC Standard 62,933 [59–61]. The Energy Storage Integration Council (ESIC) developed another energy storage test manual [40]. It also covers important efficiency metrics like usable battery capacity, nominal powers, auxiliary loads, RTE and response time and adds metrics like settling times. In addition, the guideline defines operational performance tests, meant for systems with limiting maintenance or testing intervals available. However, during this test, the energy storage system will only be tested through a single charge and discharge cycle at nominal power. The test sequence might not be sufficient to determine all important performance characteristics, since, for example, the battery capacity [62] and the dead and settling times depend on the power level [63]. Furthermore, the test manual contains special test protocols for DC-coupled PV storage systems for component and system characterization. Procedures are defined to validate the functionality and integration, as well as to measure the efficiency of the DC-DC converter attached to the battery.

Additional information and further test procedures can be found, for example, in Blair et al. [51], Vartanian et al. [53] and Choi et al. [64]. Although the previously mentioned standards and test methods contain detailed procedures for measuring important performance characteristics, it remains to be noted, that their focus is rather on typical grid applications of bigger-sized storage systems. The application area of residential PV home storage systems is different. At the same time, important performance characteristics such as conversion efficiency of the different conversion paths like PV-feed in or battery charging as well as stationary control deviations remain unconsidered.

In the following, publications are presented that explicitly aim to evaluate PV and PV battery systems. The IEC 61683 defines detailed procedures for measuring the efficiency of stand-alone or grid-connected power conditioners in PV applications [65]. The conversion efficiency is measured at different voltage levels and different ratios of the nominal output power ((5 %), 10 %, 25 %, 50 %, 75 %, 100 % and 120 %). In addition, a measuring specification for determining the standby loss is given. In 2010, the European standard EN 50530 extended the number of power levels to include supporting points at 20 % and 30 % of the nominal power in order to capture the conversion efficiency in the partial load range in more detail [66]. However, both standards focus on PV inverter systems. The power at the battery terminals during the typical operation of PV battery systems is different from PV inverter applications [45].

Methods for determining characteristic performance values of residential PV battery systems in the laboratory have been presented in various publications. The Australian research institute ITP Renewables has regularly presented test reports on the performance of several residential and commercial battery packs between 2015 and 2022 [67]. In addition to the performance tests of conventional battery technologies, emerging battery systems based on sodium-ion or zinc-bromine were also investigated. However, their main focus was on the aging-related capacity loss and RTE of the batteries. Statements about the performance of the other system components of a PV battery system cannot be derived from the studies.

Messner et al. presented specific laboratory test procedures which enable a qualitative and quantitative evaluation of the performance of residential PV battery systems in 2016 [43,68]. The authors distinguish between the energy efficiency and the effectiveness of these devices. The determination of the battery capacity and RTE is similar to the PNNL with several full cycles at different power levels. The standby consumption of the conversion system is determined within a defined period, once with a fully charged and once with a fully discharged battery [43]. In addition, test procedures similar to those in EN 50530 are presented for determining individual path efficiencies such as PV feed-in, battery charge or discharge. The effectiveness (settling time and steady-state error) of the control system is evaluated by dynamic load profiles via multiple-step responses, resulting in a continuous alternation between battery charging and discharging. A similar procedure for determining control efficiency was applied to 4 systems by Munzke et al. [69]. During the tests, the authors determined rise times, dead times and settling times, and the energy exchange with the grid.

Niedermeyer et al. used a similar measurement setup as Messner et al. and considered the EN 50350 and the IEC 61683 to determine the different path efficiencies [39]. In addition, the authors presented a method to estimate the system performance as an aggregation of the efficiency of the individual energy conversions. However, standby and control losses are not included. Therefore, Niedermeyer et al. [70] also developed a four-day application test with reference load profiles of the PV generation and household load. From the measurement results, 3 performance indicators (energy conversion, control quality and achievable self-sufficiency) were determined. For each indicator, a possible classification from A to E was proposed. An almost identical test setup was presented by Bamberger et al. in [47]. Four systems were measured over 3 days each. Based on the test results, annual parameters were extrapolated using correction factors. The application tests have the disadvantage that the measurement results are already influenced by the predefined test profiles. To what extent the test results are applicable for other use cases remains to be seen.

Kairies et al. compared the laboratory measurement results of 4 PV battery systems with different battery technologies and system topologies [71]. In addition to the conversion efficiency of the inverters and the battery, the power consumption in standby mode and the control performance (transient response and stationary control deviations) are compared. In some cases, significant differences between the systems could be identified.

Building on the experience and the measurement results of the

various testing institutes, the first version of the "Efficiency Guideline for PV storage systems" (in the following: efficiency guideline) was developed together with various manufacturers, scientists, as well as the German BSW and the German Energy Storage Association (BVES) [72]. The efficiency guideline describes the measurement procedures for the system properties listed in Table I for three different system topologies. The determination of the nominal powers for the different specific conversion paths is the basis for the subsequent performance measurements of the power conversion system and the battery storage. Furthermore, tests regarding the control deviations are conducted.

For the measurements according to the efficiency guideline, the PV home storage systems are integrated into a hardware-in-the-loop test environment. The electrical load is provided by a resistive and controllable electric AC load. The generation is given by a DC source (PV simulator) with specified conditions according to the DIN 50530. Advanced charging strategies, such as forecast-based charging [73] need to be deactivated. The current and voltage are measured at various points by sensors integrated within the test environment in an interval of at least 200 ms. Fig. 1 shows the measurement points of an AC- and DC-coupled PV battery system as defined in the efficiency guideline. At the general measurement points, which are independent of the system topology, the DC power of the PV simulator (PVS) and the battery (BAT) as well as the AC power of the emulated load (LOAD), the resulting grid power (GRID) and the AC output of the battery system (AC) are determined. In the case of AC-coupled systems, the current and voltage are additionally measured at the AC connection of the PV inverter (PV-WR) and the battery inverter (BESS). Measurements for the energy management of the system and battery aging are not part of the efficiency guideline. For this reason, these aspects are not considered in this paper. Since its first release in 2017, the document has been continuously revised and edited over the past years, resulting in a second version, which is available since July 2019. Currently, the guideline is in the process of standardization.

Büchle et al. [74] and Kulkarni et al. [63] were able to show good repeatability of the measurement results in experienced testing institutes if certain boundary conditions are met during the tests. Due to the standardization of the measurement regulations, it is now possible to derive uniform data sheet specifications from the determined laboratory measurement values, see e.g. [45,72]. This improves the comparability of PV battery systems for residential buildings. At the same time, the manufacturers can identify optimization potentials.

Based on the measurement specifications, various analyses were carried out.

Since 2016, 16 commercially available home storage systems have been tested at Karlsruhe Institute of Technology (KIT) on a permanent basis in the areas of performance and their contribution to grid stability. The battery capacity of the evaluated home storage systems varies between 2.0 kWh and 5.2 kWh [75]. In this context, Munzke et al. published numerous studies. For example, the authors analyzed the efficiency and resulting annual electrical and economic losses of 9 [76] respectively 12 systems [23]. Moreover, Munzke et al. analyzed the influence of intelligent charging strategies [77] and aging effects [32] on the electrical or economic viability of different PV battery systems.

In addition, Niedermeyer et al. tested and compared 5 PV storage systems according to the efficiency guideline and conducted an application test over several days to determine the overall system efficiency [45,78]. The results were compared with two other assessment approaches. However, three of the 5 systems were already up to three years old before the measurements started. In the joint publication by HTW Berlin, KIT and other institutes, 3 of the 16 systems measured at KIT were operated in a one-week application test [44]. In contrast to previous publications, the test results were compared with the simulation results of an identical, ideal and loss-less storage system. The calculated performance index puts the cost savings achieved by the real PV storage system (grid purchase costs minus grid feed-in revenues) in relation to the theoretical cost savings potential of the ideal PV storage system. Table II gives an overview of different publications with a comparison of laboratory measurements of several PV battery systems.

Table I
Possible test sequence according to the efficiency guideline for PV storage systems [72].

Test sequence
1) Determination of the nominal power
2) Power conversion system
a) Individual conversion pathways
b) Power consumption in standby or switched off state
3) Battery
a) Capacity efficiency
b) Efficiency
4) Control deviations of the system
a) Dynamic control deviation
b) Stationary control deviation

1.4. Contribution

The previously mentioned studies have investigated smaller and older PV battery systems of the 1st product generation and the number of systems considered was comparatively small. In the meantime, however, the manufacturers have been able to make significant improvements to their systems and the usable battery capacity installed in Germany is continuously increasing [34]. For this reason, this paper analyzes 26 different sized state-of-the-art PV battery systems. It investigates differences between the performance characteristics and their reasons in more detail than before. At the same time, mostly neglected performance characteristics such as the dependency of the battery efficiency on the battery power, the control behavior under steady-state conditions or cascading, of the power electronics are analyzed. Furthermore, the challenges of the measurements are highlighted. These are often disregarded, but important because not all tests according to the efficiency guideline can be performed smoothly on the various systems. In a concluding chapter, the so far largely neglected performance characteristics that occur in real operation but are not considered by the efficiency guideline are presented. The research questions answered in this paper are:

- What is the range of the efficiency characteristics of different sized state-of-the-art lithium-ion PV home storage systems?
- How much do the manufacturer's specifications for the usable battery capacity deviate from the laboratory test results?
- What contributes to the differences in standby power consumption and conversion losses between the systems?
- How do the systems differ in their control behavior under stationary and dynamic conditions?
- Which performance aspects are not characterized by the laboratory tests according to the efficiency guideline?

2. Efficiency characteristics

2.1. Photovoltaic home storage systems under evaluation

Since 2018 the research group solar storage systems at the university of applied science HTW Berlin has been conducting the annual energy storage inspection [30,34,79–81]. A total of 23 manufacturers with 64 different system configurations took part in the five issues to date. They were measured by several testing institutes according to the specifications of the efficiency guideline for PV storage systems [72].

This chapter compares the measurement data of 26 different state-of-the-art residential PV battery storage systems. The systems were evaluated in the annual Energy Storage Inspection between 2020 and 2022 [17,24,64]. The required laboratory tests were carried out by the independent institutes Austrian Institute of Technology (AIT) and the

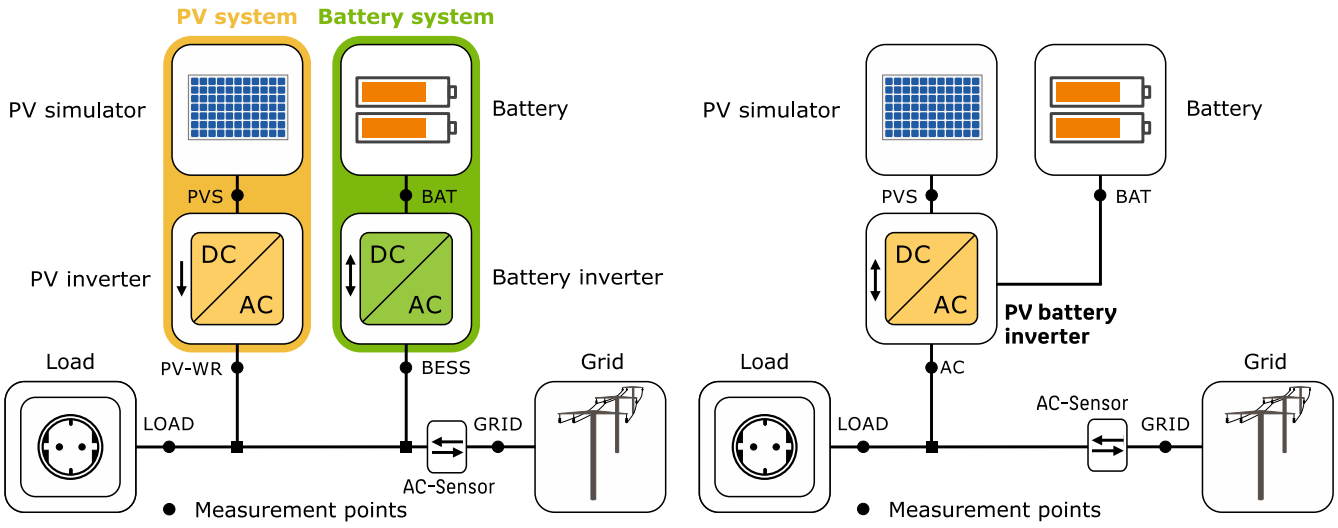

Fig. 1. Main system components as well as measuring points of AC- (left) and DC- coupled PV battery systems (right).

Table II
Overview of different publications with a comparison of laboratory measurements of several PV battery systems.

Author and year	Language	Institution	Number of systems	Battery coupling		Battery capacity range	Measurements according to the efficiency guideline	Main focus of the paper
				AC	DC			
Niedermeyer et al. [70], (2015)	German	Fraunhofer IWES, Germany	3	2	1	Not specified	No	Three performance indicators of energy efficiency, control and self-sufficiency are determined based on an application test.
Kairies et al. [71], (2016)	German	RWTH Aachen, Germany	4	2	2	2 kWh to 9.2 kWh	No	With the high-resolution measurement of 4 PV battery systems under laboratory conditions, measurements of conversion and battery efficiency, standby consumption and control deviations were published.
Messner et al. [43] (2016)	English	AIT Wien, Austria	2	–	2	Not specified	No	Overview and analysis of different test methods and comparative results of individual laboratory tests. The methods developed were intended to serve as a basis for future standardization.
Munzke et al. [76], (2017)	German	KIT, Germany	8	Not specified		2.1 kWh to 5.3 kWh	Yes	First publication of measured values according to the efficiency guideline of several PV battery systems. Calculation of various parameters such as degree of self-sufficiency and self-consumption share as well as economic losses per year.
Orth et al. [76], (2018)	German	HTW Berlin, Germany	3	2	1	3.9 kWh to 4.3 kWh	Partly (usable battery capacity)	This article presents a one-week application test that makes the efficiency of PV storage systems for single-family homes comparable. The test results were compared with the simulation results of an identical, ideal, and loss-less storage system.
Weniger et al. [79], (2018)	German	HTW Berlin, Germany	20	8	12	2.8 kWh to 11.3 kWh	Yes	The Energy Storage Inspection is an annual study that has been published in German since 2018. It compares the laboratory measurement values recorded following the efficiency guideline and ranks the systems based on a calculated performance indicator.
Niedermeyer et al. [45], (2020)	English	Fraunhofer IEE, Germany	5	3	2	2.2 kWh to 7.4	Yes	This paper presents and evaluates three different methods to determine the total PV battery system performance.
Bamberger et al. [47], (2020)	German	SPF at OST, Switzerland	4	2	2	2.3 kWh to 7.7 kWh	No	Development of a PV home storage test with which relevant operating conditions can be tested within three test days and annual characteristic values can be extrapolated.
Munzke et al. [23], (2020)	English	KIT, Germany	12	4	8	2.0 kWh to 4.6 kWh	Yes	Twelve systems are measured under identical conditions using so-called reference days. Based on this, the annual average efficiency, the system losses, and the monetary losses per year are determined.
Munzke et al. [32], (2021)	English	KIT, Germany	4	4	–	2.3 kWh to 4.0 kWh	Partly	In this paper, a sensitivity analysis is carried out on the influence of system efficiency, component aging, and charging strategy intelligence on the dimensioning and profitability of a PV home storage system.
ITP Renewables [67], (2022)	English	ITP, Australia	15	2	13	8.0 kWh to 13.5 kWh	No	The objective of the multi-year tests was to independently verify battery performance (capacity fade and round-trip efficiency) against manufacturers' claims.

Karlsruhe Institute of Technology (KIT) according to the specifications of the efficiency guideline. Table III gives an overview of the test and measurement equipment used for the acquisition of the data. The measured values recorded were documented in test reports, which form the basis for the following comparison of the different storage systems.

To distinguish the individual products, each system configuration is given an abbreviation (e.g. A1, A2, etc.). The letter varies depending on the inverter manufacturer or complete system provider. The number indicates how many system configurations were analyzed per manufacturer. Table IV shows the system abbreviation and the measurement time as well as the full product name of the different systems under study. A total of 11 manufactures have opted to label their 22 devices with the product name. However, for the devices J1 to L2 no product name is given because the manufacturer decided against mentioning it. Since no measurement of the usable battery capacity has been carried out for system D1, only the characteristics of the hybrid inverter are analyzed. In 9 of the so-called AC-coupled storage systems A1 to D4, the batteries are connected to the power grid via bidirectional battery inverters, see also Fig. 1. In contrast, the 17 DC-coupled systems D5 to L2 use a hybrid inverter that links the PV generator to the storage system and the grid. In most cases, different manufacturers produce the lithium-ion batteries and the inverters. Individual systems have the same battery inverter (e.g. D1 and D2) but have been measured with a different battery. In other system combinations, however, the hybrid inverter varies. The type of battery is the same and the number of battery modules is identical (e.g. D4, D5, D6, E2 and F1, or D3 and F2).

In the following sections, the most important efficiency related characteristics of the 26 systems are compared. Additionally, the test procedure for determining the different properties according to the efficiency guideline is described in an introductory manner.

2.2. Nominal power

The limitation of the charge and discharge power of the battery system as well as the maximum power output of the PV generator influences the operating behavior and the performance of the PV battery system.

Fig. 2 (left) illustrates the procedure for determining the nominal power using the example of the measurement of the discharge power of system D3. The electrical load applied to the system is continuously increased in the test laboratory with the PV simulator deactivated. To cover the demand, the battery system discharges. The difference between the electrical load and the discharge power is primarily due to the conversion losses in the battery inverter. However, it may also be associated with stationary control deviations. According to the test specifications of the efficiency guideline, the nominal power is reached when the battery power stagnates while the electrical load continues to increase. In this case, a nominal DC discharge power of 10.4 kW was

Table III
Overview of the test and measurement equipment used; [1] Version 1.1 for system C1 (see Table IV).

AIT	
AC load	AIT load cascade V1.0[1]
PV simulator	AIT PVAS3
Measurement equipment	DEWETRON 808 *or* DEWESOFT SIRIUS measurement system *with* LEM IT 200-S *or* 205-S Ultrastab current transducer ULTRASTAB

KIT	
AC load	Höcherl & Hackl 3× ZSAC2826
PV simulator	Regatron: 2× TopCon TC.P.10.1000.400.S and 2× TC.LIN. SER.40.1000.40 *or* 2× Spitzenberger & Spieß PVS10.000
Measurement equipment	Zimmer LMG 670

Table IV
System abbreviation, measurement time and product names of the systems under study.

Abbrev.	Measurement time	Product name of the fully integrated system	Product name of the inverter	Product name of the battery
A1	JAN. 2020	–	SMA Sunny Boy Storage 5.0	IBC Solar era: powerbase 15.0 HV
B1	DEZ. 2019	VARTA pulse 6	–	–
B2	DEZ. 2019	VARTA pulse 6 neo and VARTA pulse 6	–	–
B3	JAN. 2021	VARTA pulse 6 neo	–	–
C1	APR. 2021	sonnen sonnenBatterie 10	–	–
D1	OCT. 2019	–	KOSTAL PLENTICORE BI 5.5	BYD Battery-Box H9.0
D2	OCT. 2019	–	KOSTAL PLENTICORE BI 5.5	BYD Battery-Box H11.5
D3	APR. 2021	–	KOSTAL PLENTICORE BI 10/26	BYD Battery-Box Premium HVS 12.8
D4	MAR. 2021	–	KOSTAL PIKO MP plus 4.6–2 (AC)	BYD Battery-Box Premium HVS 7.7
D5	APR. 2021	–	KOSTAL PIKO MP plus 4.6–2 (DC)	BYD Battery-Box Premium HVS 7.7
D6	APR. 2021	–	KOSTAL PLENTICORE plus 5.5	BYD Battery-Box Premium HVS 7.7
D7	APR. 2021	–	KOSTAL PLENTICORE plus 10	BYD Battery-Box Premium HVS 12.8
E1	NOV. 2019	–	Fronius Symo GEN24 10.0 Plus	BYD Battery-Box H11.5
E2	APR. 2021	–	Fronius Primo GEN24 6.0 Plus	BYD Battery-Box Premium HVS 7.7
E3	APR. 2021	–	Fronius Symo GEN24 10.0 Plus	BYD Battery-Box Premium HVS 10.2
F1	APR. 2021	–	GoodWe GW5000-EH	BYD Battery-Box Premium HVS 7.7
F2	APR. 2021	–	GoodWe GW10K-ET	BYD Battery-Box Premium HVS 12.8
G1	FEB. 2021	–	RCT Power Power Storage DC 6.0	RCT Power Battery 7.6
G2	FEB. 2021	–	RCT Power Power Storage DC 10.0	RCT Power Battery 11.5
H1	JAN. 2022	Fenecon Home	–	–
I1	APR. 2021	E3/DC S10 E INFINITY	–	–
I2	APR. 2021	E3/DC S10 X COMPACT	–	–
J1	JAN. 2020	DC-coupled system of an anonymous participant		
K1	APR. 2021	DC-coupled system of an anonymous participant		
L1	JAN. 2022	DC-coupled system of an anonymous participant		
L2	JAN. 2022	DC-coupled system of an anonymous participant		

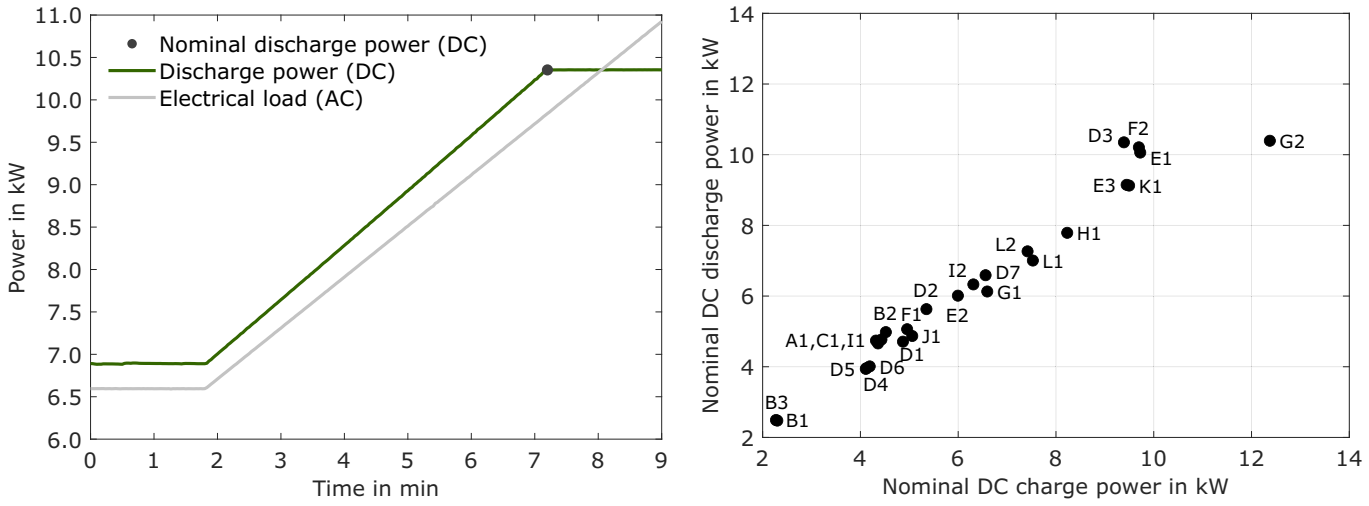

Fig. 2. Determination of the nominal discharge power (left) of the battery storage by the continuous increase of the electrical load demand (example: system D3). Nominal DC discharge and charge power (right) of the analyzed systems.

determined for system D3.

Fig. 2 (right) depicts the nominal DC charge and discharge power of the analyzed systems. These often differ only slightly from each other. Systems B1 and B3 have the lowest maximum charge power of 2.3 kW, while system G2 has the highest of 12.4 kW. However, not all systems can provide the nominal charge power at short notice. This can have a negative impact, especially on days with highly fluctuating cloud cover. Power electronics that are not well sized and too small or too large can have various disadvantages. For example, if the charge power is too low, it may not be possible to store the entire PV energy surplus. In contrast, the limitation of the battery discharge power results in peak loads only partially covered by the battery. These characteristics are especially significant when a large battery is connected to small power electronics. Usually, the energy throughput of the battery decreases the lower its maximum charge and discharge power is [82]. However, oversizing of the power electronics can result in higher efficiency losses especially in the lower power range [23].

In almost half of the systems, the nominal discharge power is less than 5 kW. Only five of the 26 analyzed systems can handle load peaks above 8 kW. Systems D3 and G2 have the highest discharge power with 10.4 kW. The discharge power of the system G2 is about 2 kW lower than its charge power. This is due to the lower maximum current and the lower battery voltage during discharging. In the case of the high voltage systems D1 and D2, which have an identical battery inverter, the discharge power increases with rising battery voltage and consequently with increasing battery capacity. In contrast, the battery unit is identical for the systems D3 and D7 as well as for D6, E2 and F1. Here, the different current limitations of the battery converters and hybrid inverters determine the resulting nominal discharge power. The ratio of discharge power to usable storage capacity (often called C-rate) varies between 0.3 kW/kWh (A1) and 1.0 kW/kWh (E1), see also Table VII in the appendix.

For individual systems, a dependence of the battery power on the battery voltage and therefore on the state of charge (SOC) can be identified. Fig. 3 shows the discharge power and battery voltage of system E3 during a complete discharge process. According to the efficiency guideline, the nominal battery power needs to be determined at average SOC. To cover the load, the system is discharged and the battery voltage drops. Since the battery current is limited by the power electronics of the inverter to 22 A, the power decreases with the voltage. System E3 can therefore deliver a maximum of 9.4 kW when the battery is fully charged and only 8.9 kW at the end of the discharge process. The nominal DC discharge power at a SOC of 57 % and 416 V is 9.2 kW.

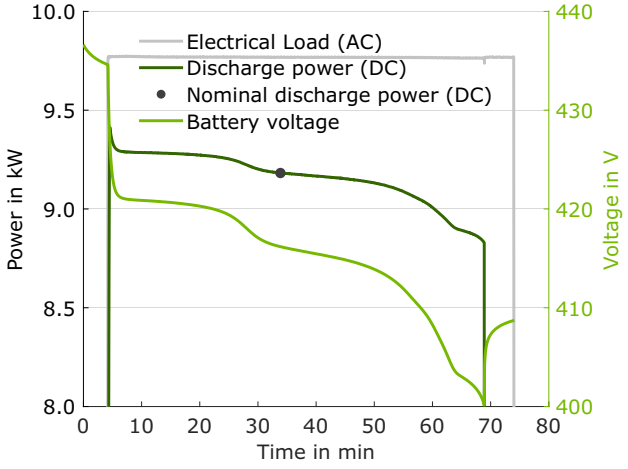

Fig. 3. Dependence of the discharge power on the battery voltage (example: system E3).

Similar behavior can be observed when charging with PV power or grid power. Here, however, the charge power increases with the battery voltage as long as the maximum input current of the inverter is the limiting factor.

Apart from the previously mentioned situation, a dependence of the nominal power on the battery voltage can also exist if the open-circuit constant voltage curve of the battery cells has a larger slope over the mean SOC range which is relevant for the guideline measurements [74]. Problems can arise, especially at high C-rates, because the required average SOC is quickly abandoned. For this reason, the measurements are sometimes triggered with an initial state of charge just below (charging situation) or slightly above (discharging situation) the average value [78]. Regardless of the situation, during subsequent measurements of the conversion efficiency at nominal power, it must be ensured that these measurements are carried out at the same battery voltage.

In addition, the maximum power output of the PV generator is limited by the PV inverter used in AC-coupled systems. Whereas in DC-coupled systems the nominal PV input power is the limiting factor. As shown in Table V the nominal PV input power of the analyzed DC-coupled systems varies between 4.7 kW (D5) and 12.7 kW (I1). The hybrid inverters of the smaller sized DC-coupled systems D5, D6, E2, F1,

Table V
Nominal PV input power (DC) of the DC-coupled systems.

System	D5	D6	D7	E1	E2	E3	F1	F2	G1	G2	H1	I1	I2	J1	K1	L1	L2
Power in kW	4.7	5.7	10.3	10.2	6.3	10.5	5.2	10.4	6.2	10.4	10.3	12.7	12.6	10.3	11.4	10.3	11.5

and G1 can handle a PV output of around 5 kW to 6 kW. The other systems are more suitable for combination with double sized PV systems. Finally, it should be noted that the resulting sizing losses of different PV home storage systems are strongly affected by the daily course of the PV production, as well as by the applications the household is equipped with (e.g. heat pump or electric vehicle) and the resulting power demand [82,83].

2.3. Usable battery capacity

The main objective of a PV home storage system is to minimize the amount of energy drawn from the grid. Therefore, the amount of energy that can be stored during the day to be used in the evening to meet the household's electricity demand is crucial. The energy provided by the battery system strongly depends on its usable battery capacity. It corresponds to the energy output of the battery during discharging. To determine the usable battery capacity as well as the battery efficiency, the storage system is fully charged and discharged several times in the laboratory.

Fig. 4 shows the measurement results of the battery test conducted by KIT for system D3. The initial state for this test is a fully charged battery. The first charging process is not displayed as it starts from an unknown SOC. In the first step, energy is drawn from the system at nominal discharge power (10.4 kW) by applying a constant load and no generation. Afterwards, the battery is recharged at nominal charge power (9.4 kW) by specifying a constant generation. Thus, the system runs through a so-called full cycle; the energy quantities are recorded for each charging and discharging process. The battery is considered to be fully charged or discharged, if the battery power falls below 1 % of the nominal charge or discharge power for 5 min, despite available DC input power or load being applied [72]. If this threshold value is not undercut, the battery is considered to be fully charged as soon as the battery charge power has fallen below 3 % of the nominal charge power over a period of 1 h [72]. Afterwards, this test is repeated at 50 % and 25 % of the nominal charge and discharge power. Due to the lower power values the duration of the different charge and discharge processes increases. To determine the usable battery capacity, the battery must go through a minimum of 3 full cycles for each of the 3 different power levels. The

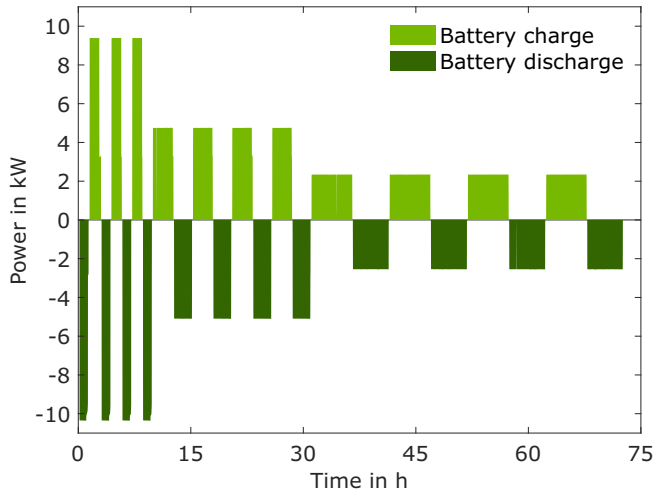

Fig. 4. Charge and discharge power of the battery storage system during the test to determine the usable battery capacity (example: system D3).

testing time depends on the system size but is usually mainly responsible for the duration of the entire laboratory test. The lower the ratio of nominal power to usable battery capacity, the longer it takes. Finally, the usable battery capacity is determined from the average value delivered on the DC side of multiple full cycles. In this example, only the 3rd and 4th full cycles of each power level are used to calculate the average values. The first cycles usually serve only as preconditioning, since the battery behavior may depend on the conditions of the previous cycle.

Fig. 5 (top) shows the usable battery capacities of the analyzed systems determined within the laboratory tests. They vary between 5.8 kWh (B1 and B3) and 16.7 kWh (K1). Approximately half of the devices have a usable battery capacity of more than 10 kWh. Another 9 systems are in the range between 7 kWh and 10 kWh. Thus, the average battery capacity of the analyzed systems (10.4 kWh) is higher than the average capacity of the PV home storage systems installed in Germany in 2021 of about 8.8 kWh [12]. However, the development of home storage batteries towards higher battery capacities has already been evident for several years [38,84]. This can be explained, for example, by the use of larger battery modules. One example is the new Battery-Box Premium HVS product line from BYD which has twice as much battery capacity per battery module compared to the previous series (used in D1 and D2). Furthermore, larger battery cells are increasingly being used in terms of capacity. Due to their series connection, the resulting battery voltage per kWh battery capacity decreases. However, to achieve the minimum input voltage specified by the inverters, batteries with higher battery capacities are required.

The modular system concepts D3 to D7 and E2 to F2 participated with the BYD Battery-Box Premium HVS. Depending on the system configuration, these systems were tested with 3 to 5 battery modules connected in series, resulting in usable battery capacities between 7.0 kWh and 12.3 kWh. At the same time, several systems were measured with the same type of battery and number of battery modules, see Table IV. This applies, for example, to the systems D4, D5, D6, E2 and F1. For 4 of these 5 systems, usable battery capacities of 7.3 kWh or 7.4 kWh and thus small capacity differences were determined. For system D6, the usable battery capacity of 7.1 kWh deviates by around 3 % from the other measurement values. In this case, the KIT observed that the discharging processes ended at different battery voltages. This resulted in an approximately 10 % lower DC energy output of the battery storage for 2 full cycles. The reason for the differences could not be conclusively explained, but an incorrect SOC determination of the device under test could be responsible.

Furthermore, the energy that can be discharged from the battery depends on the nominal charge and discharge power [74]. This is partly the reason for the differences in the usable battery capacity of the systems D3, D7 and F2. Therefore, battery data sheets should indicate that the usable battery capacity depends on the inverter and its power rating.

For systems G1 and G2, the cycle tests were only carried out with 50 % and 25 % of the nominal charge and discharge power. The complete charging and discharging of the battery systems with nominal power were not possible due to a temperature-related shutdown. The battery management system (BMS) reduced the current because the maximum permissible cell temperatures were exceeded. Multiple cycling at full power is the greatest stress test in terms of temperature. This is also the reason why system L1 was measured at the highest power levels with 75 % instead of 100 % of the nominal charge and discharge power. However, in real operation, the systems are rarely operated in this way, which means that the high temperatures are usually not achieved.

Fig. 5 (bottom) compares the percentage deviation between the

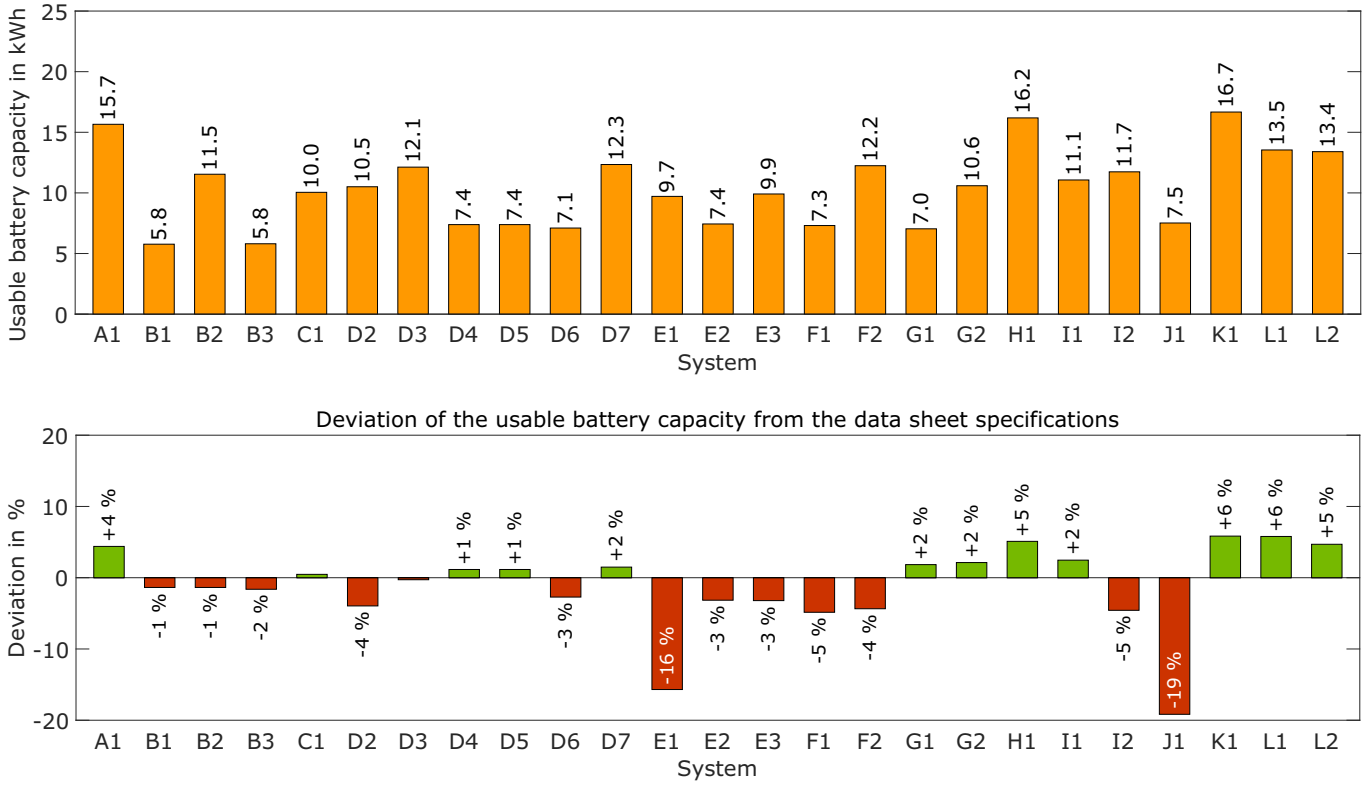

Fig. 5. Comparison of the usable battery capacities (top) of the analyzed systems, D1: measured data of the battery are not available. Difference between the laboratory measurements (bottom) and data sheet values of the usable battery capacities (positive deviation: measured value greater than data sheet value, negative deviation: measured value smaller than data sheet value).

measured usable battery capacity and that stated in the data sheet specifications for the systems under study. With the exception of systems D2 to D7 and H1, the data sheets of the battery suppliers were used for the analysis. The two inverter manufacturers D and H refer to a limited usable battery capacity in their data sheets. For manufacturer L, the characteristic value could only be taken from the operating and installation instructions. The deviations range from −19 % to +6 %. Lower usable battery capacities were determined for 12 of the 25 systems in the laboratory test.

Inverter and battery suppliers often deliberately restrict the depth of discharge (DOD). In most of the systems studied, the DOD is around 95 %. The DOD restriction serves, in particular, to protect the battery against deep discharge. By limiting the DOD, especially calendar aging caused by high voltage respectively SOC levels can be reduced [85–87]. Some manufacturers specify the usable battery capacity with a DOD of 100 % although, for example, only a DOD of 95 % is permissible in operation. It should be noted, that the measurement results may also be influenced by the quality of the SOC determination of the systems and the testing conditions of the laboratories or battery manufacturers [43,63]. Büchle et al., for example, were able to show a significant dependence of the discharged energy on the ambient temperature [74]. Charge and discharge resistances increase with decreasing temperature due to the slow-down of electrochemical and physical processes [88]. Another reason for the capacity differences may be preconditioning. Depending on the preconditioning process of the battery storage, the initial charge balancing between the battery cells may not have been completed at the time of the laboratory tests.

2.4. Conversion efficiency

2.4.1. Battery efficiency

Any energy conversion within the system's power electronic

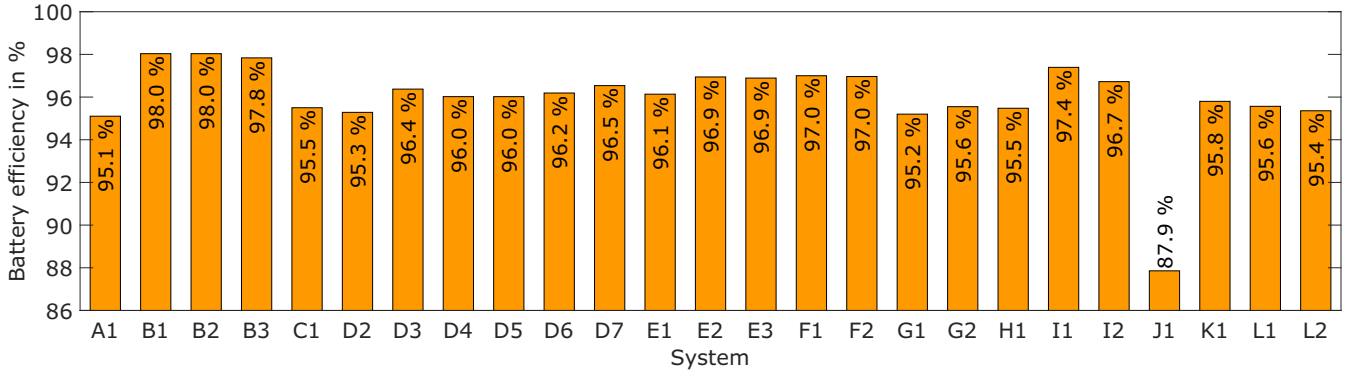

Fig. 6. Average battery efficiency of the analyzed systems.

components and in the battery results in losses. Fig. 6 compares the battery efficiency of the battery storage systems under study. They correspond to the ratio of the DC energy discharged from the battery to the DC energy charged. These energy quantities were determined during the full cycle tests described in Section 2.3 at different power levels. The battery efficiencies shown in Fig. 6 correspond to the mean value from the measurement results of the 2nd and 3rd full cycles per power level. The battery efficiencies vary up to 10 percentage points between 87.9 % and 98.0 %.

The battery modules of LG Energy Solution installed in the systems of the manufacturers B and I1 show the least losses. The battery modules from the manufacturers Samsung (I2) and BYD (D2 to F2) generally achieve efficiencies above 96 %. Only the predecessor model of the BYD HVS series in system D2 falls slightly short with 95.3 %. The low battery efficiency of system J1 can be especially attributed to the DC-DC converter integrated into the battery storage system. The external clamp voltage of the battery can thus be largely decoupled from the internal battery voltage resulting from the interconnection of the battery cells. In charging mode, the DC-DC converter works as a buck converter and in discharging mode as a boost converter. However, balancing the voltage differences results in additional conversion losses, which significantly reduce the efficiency of the battery. The average conversion efficiency of the analyzed lithium-ion batteries is 96.0 % and the median is 96.1 %. The reasons for the differences in battery efficiency are diverse. They depend on the system, the electrical interconnection, the quality of the battery cells, as well as the fact that the cell chemistry of the batteries is different [75]. In addition, the power consumption of the BMS during the charging and discharging process can have a decisive influence on battery efficiency [43].

The battery efficiency as well as the available battery capacity depend on the charge and discharge power [62]. Generally, the battery efficiency decreases with increasing charge and discharge power, see Fig. 7 and e.g. [71,78]. This behavior can be observed in the depicted example systems B3, D7, I2 and K1. System I2 has the largest difference of 2.2 percentage points between the lowest and highest battery power level. The differences in battery efficiency can be explained, among other things, by the voltage drop across the internal resistance of the battery, which results from the various charging and discharging currents of the 3 power levels. The battery efficiency increases with decreasing charge and discharge power, which results from the associated lower charge energy and a proportionally higher discharging energy per cycle iteration occurs [74]. In other systems (e.g. A1 and D7), the highest efficiency is achieved in the medium power range. Especially during long test periods with low power (25 %), the constant

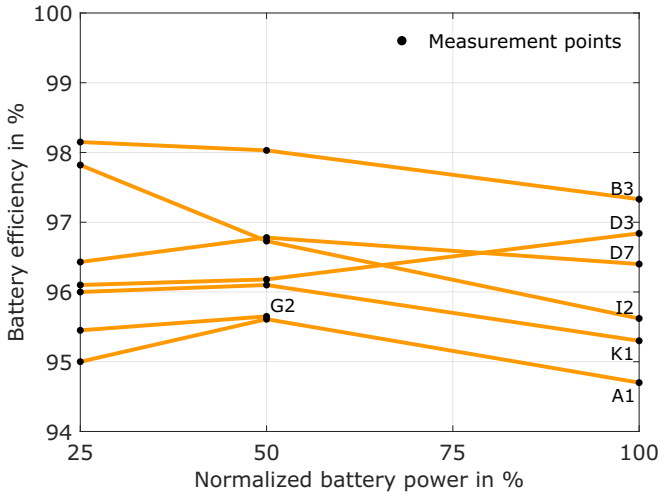

Fig. 7. Battery power dependency of the battery efficiency of 7 example systems. For better readability of the graph, not all systems investigated are shown.

consumption to supply internal loads, e.g. a display or to cover the BMS consumption, is significant and can reduce the battery efficiency [78]. Although the same battery has been measured in systems D3, D7 and F2, a contrary behavior can be observed. In system D3, the battery efficiency increases with the charge and discharge power. This may be attributed to a different settling behavior in some cycles and an associated variation in the final charge voltage. However, the exact cause has not yet been clarified. As mentioned above, the full cycle test on system G2 could not be performed at full power.

2.4.2. *Efficiency of the power conversion system*

The type of power electronic integration of the battery determines the concept name, the individual system components, the measuring points and the energy conversion paths. Primarily, a distinction can be made between the market-relevant AC- and DC-coupled PV home storage systems. Fig. 8 (top) illustrates the individual energy conversion paths of the two system topologies. Furthermore, the picture shows the abbreviations of the measuring points, which serve to describe the energy conversion paths. The path abbreviations are named according to the direction of the energy flow from the source to the sink. For example, the pathway PV2AC describes the conversion of the DC power output of the PV generator into grid-compliant AC power. In AC-coupled systems, the associated losses occur in the separate PV inverter. Moreover, there are conversion losses in the bidirectional battery inverter during charging (AC2BAT) and discharging (BAT2AC). The independent installation of the PV generator and the battery enables the option to size every part of the system independently, without the limitations of one over the others [89]. In contrast, DC-coupled systems combine all power electronic components in one device. Here, the PV generator and the battery are connected to the DC link of the PV battery inverter via DC-DC-converters [45]. Thus, the losses of the PV2AC, PV2BAT and BAT2AC conversion paths occur in the PV battery inverter. Some DC-coupled systems can additionally be charged with energy from the AC side (AC2BAT). In these cases, the inverter bridge of the device is bidirectional. This allows the battery to be recharged with energy from the grid if this is necessary, for example, to protect itself from deep discharge [90].

Since the conversion efficiency of the inverters is significantly influenced by the input power and the DC input voltage [91], the voltage levels of the different systems will be analyzed in the following. Fig. 8 (bottom) illustrates the battery voltage range, which is determined by the minimum and the maximum permissible battery voltage. In the systems B1 to B3 as well as I1, low voltage batteries with a nominal voltage of 52 V are integrated. In contrast, the 22 high voltage systems have nominal battery voltages between 205 V and 512 V. With increasing nominal battery voltage, the difference between the minimum and the maximum battery voltage rises. Comparing systems D1 and D2, only the number of battery modules connected in series varies, which is the reason why the battery voltage also increases with increasing battery capacity.

Furthermore, the nominal PV input voltage of the DC-coupled systems D5 to L2 is shown in Fig. 8 (bottom). Depending on whether the connection of the battery inverter to the grid is single-phase or three-phase symmetrical, a DC link voltage of the inverter of at least 350 V or 600 V is required [92]. The highest inverter efficiencies are achieved at input voltages close to the internal DC link voltage of the inverter [91]. Therefore, the nominal PV input voltage defined by the manufacturer is often nearly identical to the DC link voltage of the inverter. The nominal PV input voltage for the three-phase PV battery inverters of the DC-coupled systems is between 570 V and 740 V. In comparison, the single-phase inverters of systems D5, E2, and F1 have a nominal PV input voltage of only 380 V to 400 V. Moreover, the voltage difference between the battery and DC link affects the required power electronic circuitry of the systems [93]. Transformer-based voltage adjustment is usually required to integrate low voltage batteries [92,93]. Therefore, low voltage batteries in AC-coupled systems are often connected to the

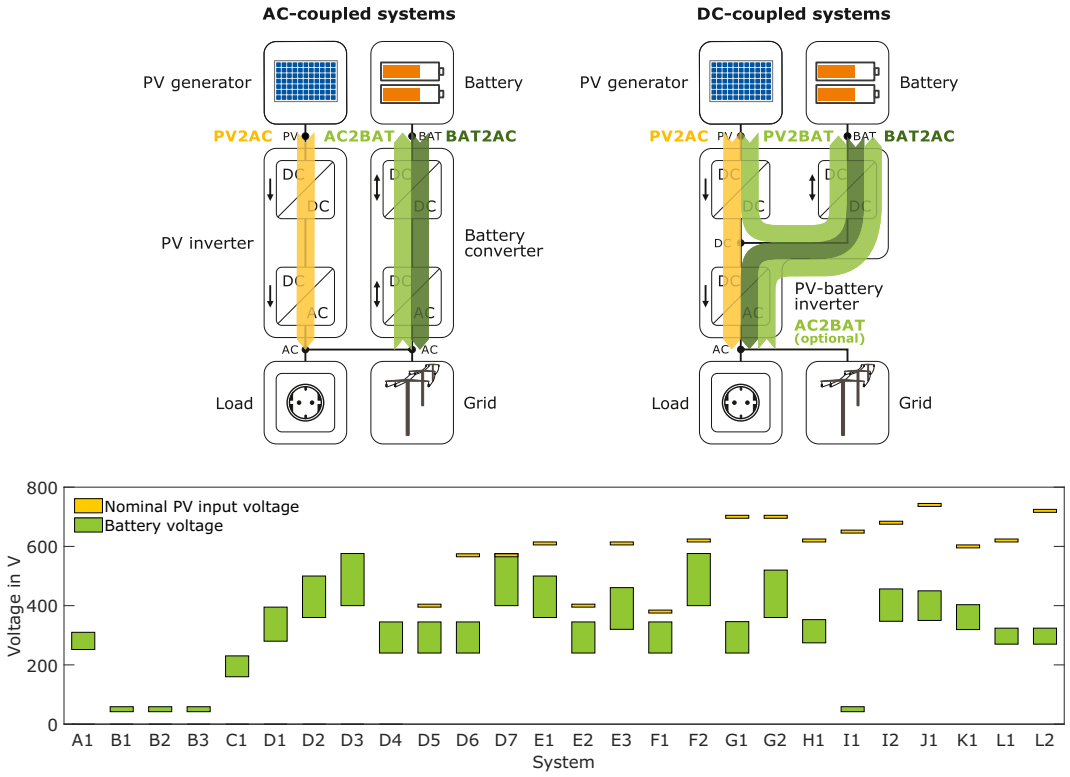

Fig. 8. Components and energy conversion pathways of AC-coupled (top left) and DC-coupled PV battery systems (top right). Battery voltage range of the analyzed system configurations as well as the nominal PV input voltage of the DC-coupled systems (bottom).

AC grid via an inverter bridge in combination with a low-frequency transformer [43]. In DC-coupled systems, a transformer-based DC-DC converter is normally used to overcome the big voltage difference via the winding ratio [94]. In contrast, high voltage batteries can be connected via a bidirectional DC-DC converter that acts as a boost or buck converter [93]. Generally, the smaller the voltage difference between the battery storage and the DC link, the higher the conversion efficiency of the power electronics during charging and discharging [63,95].

In order to be able to compare the conversion losses in the power electronic system, the efficiency guideline defines a procedure to identify the efficiencies of the paths shown in Fig. 8 (top). Again, a dependency on the applied power can be identified and therefore the conversion efficiency at different power levels has to be determined. Here, step profiles at different power levels are used [72]. Fig. 9 (left) illustrates the procedure to determine the power-dependent conversion efficiencies in the discharge mode of the inverters based on the measurement results of system D3. Since the battery voltage influences the measurement results, the voltage dependency on the SOC has to be taken into account [45]. The efficiency guideline calls for a medium SOC for most measurements, as they are easier to implement in a generalized test procedure [78]. However, to determine the efficiency of the PV feed-in energy conversion path, the battery system needs to be fully charged and

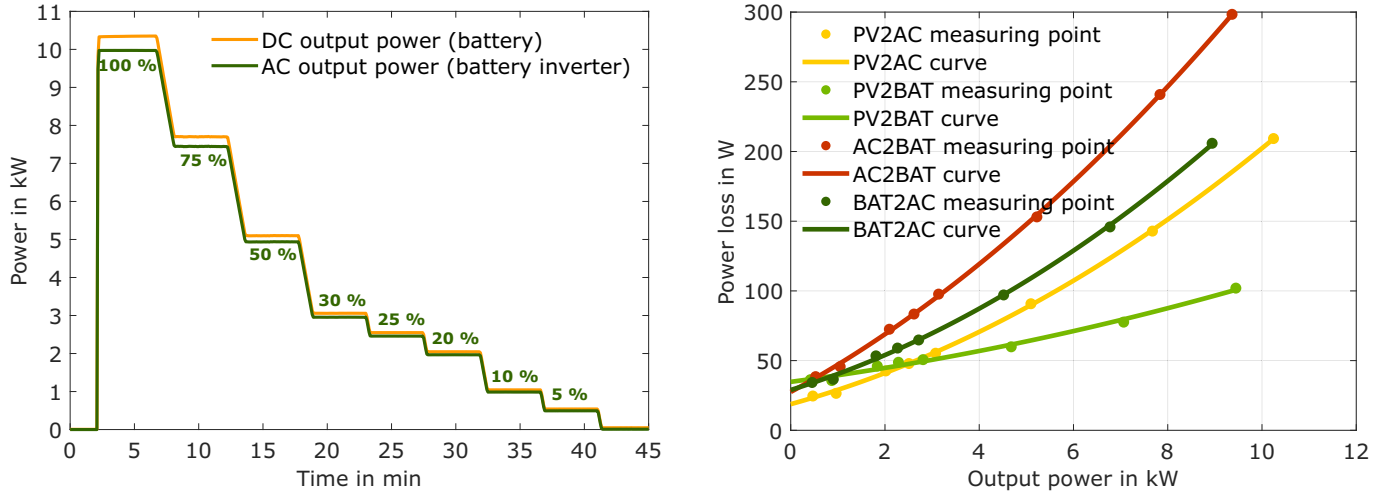

Fig. 9. AC and DC power measurements (left) during the test to determine the power-dependent conversion efficiency of a battery inverter during discharging (example: system E3). Power loss measurements and quadratic fit function (right) of the different conversion paths (system E3) as a function of the specific output power.

in standby mode. The efficiency guideline specifies that the measurements must be performed at 8 different power levels between 5 % and 100 % of the nominal output power. This results in a step profile with 8 different supporting points, see Fig. 9 (left). In contrast to IEC 61683, which focuses on PV inverters, the test procedures of EN 50530, as well as the efficiency guideline, include additional steps at 20 % and 30 % of the nominal power of the different conversion paths [66]. This procedure leads to a better coverage of the important partial load range.

To determine the discharge efficiencies, the system is applied with an electrical load high enough to deliver its nominal power over a period of around 3 min. The system has 40 s at its disposal to reach a steady state. For the determination of the average conversion efficiency, only the last 140 s are taken into account. Subsequently, the load and thus the power output of the battery system is stepwise reduced. The differences between the power output on the DC and AC sides of the system components can be attributed to the losses of the inverter. At higher power levels, the absolute values of the power loss are the highest.

The resulting power loss can be determined from the efficiency and the input power or from the difference between the input and output power. Fig. 9 (right) shows the power loss as a function of the output power for the different conversion paths of the DC-coupled system E3. In the laboratory, the 8 supporting points cannot always be set exactly due to the peculiarities of the systems and stochastic deviations. However, in most cases, the power dependence of the power loss can be described sufficiently accurately by a quadratic equation [96]. The lower power range is dominated by idling losses, which are mainly responsible for the low conversion efficiency of the inverters at partial load. Depending on the conversion path, the idle losses in system E3 vary between 19 W and 35 W. The highest losses can be identified in the PV2BAT path and the lowest during PV feed-in. With increasing power, the voltage and ohmic losses of the power electronic components become more important, which increase linearly respectively quadratically with the power throughput [97,98]. Since these losses are comparatively low for the PV2BAT path of system E3, the PV2BAT power loss is lowest compared to the other paths starting at about 25 % (around 3 kW) of the respective specific output power. With increasing power, the power losses of the PV2AC and BAT2AC paths increase almost equally, which is primarily due to the same power flow direction and the associated conversion of the DC to AC power. However, the higher losses during battery discharge are due to the comparatively higher voltage difference to the DC link voltage of the inverter. As already shown in Fig. 8 (bottom), the nominal PV voltage is higher than the battery voltage and closer to the DC link voltage of the three-phase inverter. Fig. 9 (right) shows that at full load, the losses of AC battery charging are about three times higher than the losses of direct battery charging with PV power. Finally, the quadratic function can be used to determine the conversion efficiency as a function of the input or output power.

Fig. 10 shows the resulting efficiency curves of the different

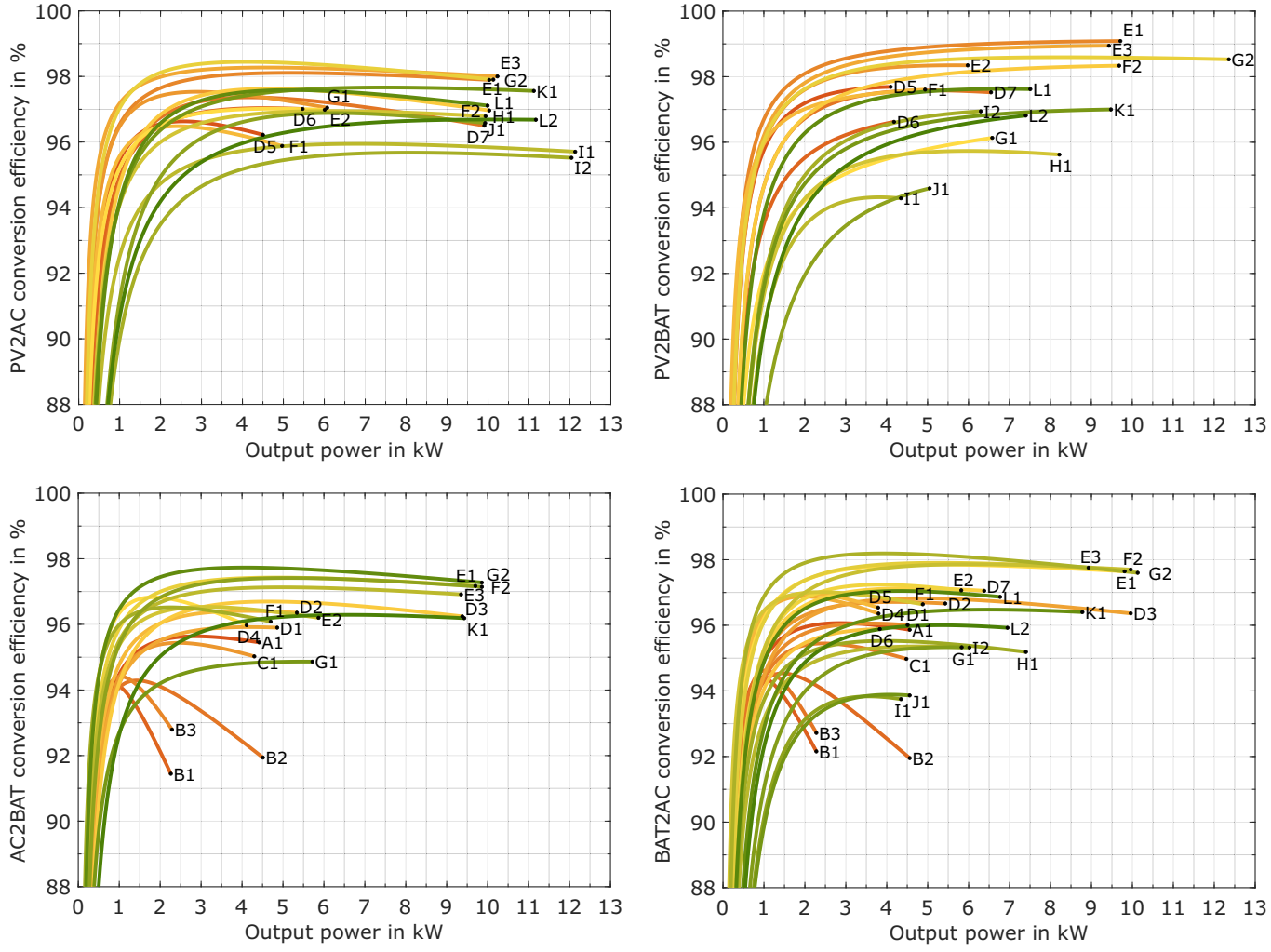

Fig. 10. PV feed-in (top left) pathway efficiency (PV2AC) of the DC-coupled systems. PV battery charging (top right) pathway efficiency (PV2BAT) of the DC-coupled systems. AC battery charging (bottom left) pathway efficiency (AC2BAT) of the AC-coupled systems and the in this regard capable DC-coupled systems E1 to G2 and K1. AC battery discharging (bottom right) pathway efficiency (BAT2AC) of the AC- and DC-coupled systems.

conversion paths as a function of the output power. The path efficiencies PV2AC and PV2BAT were determined according to the efficiency guideline at nominal PV input voltage. Furthermore, the losses due to inaccurate MPP tracking are included in the pictured conversion efficiencies of the paths PV2AC and PV2BAT and thus not analyzed separately. The efficiency curves of the paths PV2BAT, AC2BAT, and BAT2AC were recorded at a medium SOC. For comparability, the different system abbreviations were assigned to the efficiency curves at the respective nominal output power and the corresponding value of the efficiency.

At nominal output power the PV2AC efficiency of the systems studied varies between 95.5 % (I2) and 98.0 % (E3), see Fig. 10 (top left). Depending on the design of the power electronics, the efficiency increases or decreases at lower loads. However, most systems achieve nearly identical efficiencies even at a quarter of the nominal power. With the increasing importance of the idle losses in the lower power range, the conversion efficiencies drop significantly for output powers below 1 kW. The PV2AC conversion efficiency of the systems I2, J1 and L2 decreases to about 84 % at a load of 0.5 kW. At the same time, the efficiency of the systems E1 to E3 and G2 is above 94 %. The efficiency gap of 11.9 percentage points between the systems I2 and E3 can be attributed in particular to the difference in the idling losses, which differ by a factor of 4.

The PV2BAT efficiency describes the conversion efficiency of the DC-coupled systems in charging mode. Fig. 10 (top right) compares the resulting efficiency curves as a function of the output power. Under full load at maximum charging power, the PV2BAT efficiencies vary between 94.3 % (I1) and 99.1 % (E1). In contrast to the PV2AC path efficiencies, the PV2BAT efficiencies drop sooner with decreasing power, especially for the systems J1, G1, and L2. Up to a charging power of 0.5 kW, system F1 has the lowest charging losses. Above this power, E1 has the highest charging efficiency. For about half of the DC-coupled systems, the PV2BAT efficiencies are higher than the PV2AC efficiencies, especially in the upper power range. This can be explained by the lower power loss and the associated smaller voltage and ohmic losses, see also Fig. 9 (right).

The AC2BAT efficiency describes the conversion efficiency of the AC-coupled systems in charging mode or of the DC-coupled systems when charging from the grid. The comparison of the AC2BAT efficiency curves shown in Fig. 10 (bottom left) illustrates the decrease in efficiency of the low voltage systems B1 to B3 in the upper power range. This can be attributed in particular to the high switching and ohmic losses within the battery inverters. Therefore, the low voltage battery inverters reach their maximum efficiency between a quarter and half of the nominal charge power. Systems D1 and D2 are equipped with the same battery inverter but with a different battery capacity of the same battery type. Compared to system D1, the voltage difference between the battery storage and the DC link is lower in system D2 due to the higher number of battery modules connected in series. The efficiency difference of up to 0.7 percentage points between these two systems can therefore be attributed to the difference in battery voltage.

Fig. 10 (bottom right) shows the discharge efficiency (BAT2AC) for all systems under study. For most AC-coupled systems, the AC2BAT and BAT2AC efficiency curves differ only slightly from each other. At maximum discharge power, the conversion efficiencies vary between 92.0 % (B2) and 97.7 % (E1). However, numerous studies have already shown that, in contrast to the charging mode, the systems are mostly discharged with powers below 1 kW [23,82,99]. Therefore, high conversion efficiencies at partial load are important for the efficient system operation of PV home storage systems. At an AC power output of 0.5 kW, the analyzed systems achieve BAT2AC efficiencies between 83.7 % (J1) and 95.0 % (F1). The results also show that the AC-coupled systems perform well in this load range with efficiencies between 91.0 % (D3) and 94.4 % (D4). In order to achieve higher efficiencies, especially in the partial load range, power semiconductors made of silicon carbide are a promising trend for power electronic components [98]. According to manufacturers E and G, these were already used in their systems E3 and G2 [37,100].

When interpreting the conversion efficiencies, it is important to note that a discontinuously shaped efficiency curve cannot be depicted exactly using the quadratic approach [101]. This case can occasionally occur, for example, in systems that switch certain components on or off depending on the level of loading. In conjunction with the VARTA pulse 6 neo, up to five VARTA pulse energy storage units can be coupled. In the system combination B2, the pulse 6 neo and the pulse 6 (B1) are operated in cascade, which adds up their usable battery capacity as well as their output power. Here, the control of the pulse 6 neo serves as the primary controller. Fig. 11 shows the 8 measuring points and the efficiency curves of the systems B1 and B2. While the measurement points are well represented by the quadratic fit for system B1, they deviate more strongly for system B2 between 1.2 kW and 2.4 kW. In operation, system B2 follows the conversion efficiency of the pulse 6 (B1) in the lower power range up to its nominal discharge power of 2.3 kW. In order to be able to provide higher output powers, both subsystems of the cascade are operated with reduced power, in their own partial load range. For example, to provide 4 kW, both units are discharged with 2 kW. The efficiency of the cascade then corresponds to the efficiency of the individual systems at the corresponding specific load. Accordingly, the discharge efficiencies of system B2 at a specific load between 50 % and 100 % are almost identical to those of system B1. Moreover, the figure shows different fitting approaches to represent the load-dependent interconnection of the two systems. In addition to the quadratic curve fitting, the efficiency guideline offers the possibility of shape-preserving interpolation. Here, the Piecewise Cubic Hermite Interpolating Polynomial (PCHIP) method was used. However, both approaches cannot accurately represent the conversion behavior of the system. Therefore, the BAT2AC conversion efficiency is overestimated at the output powers between 1.2 kW and 2.3 kW. With an increase in the number of measurement points, the PCHIP method would have advantages over the quadratic curve fitting.

In order to be able to compare the conversion efficiency of different storage systems more easily, the so-called average path efficiencies were introduced within the second version of the efficiency guideline [72]. Here, the efficiencies for each energy conversion path are aggregated into one value. From the quadratic equation of the power loss, the conversion efficiency is calculated at 10 supporting points, which are equally distributed between 5 % and 95 % of the nominal output power, see Fig. 12 (right). The arithmetic mean of these 10 values results in the average conversion efficiency. Fig. 12 (left) shows the average efficiency

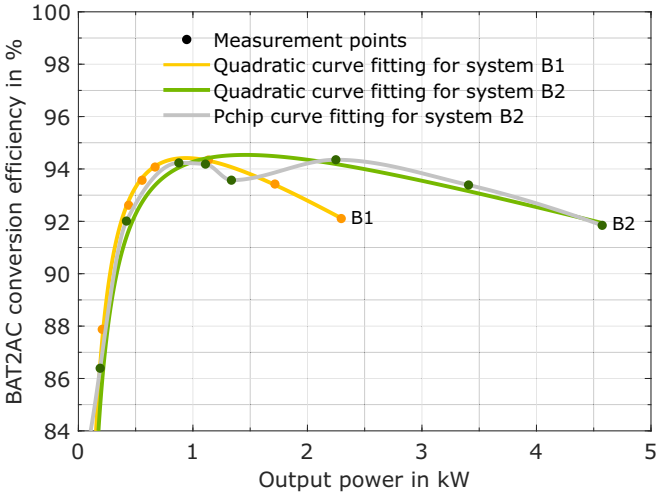

Fig. 11. Measurement points and AC battery discharging efficiency curve (BAT2AC) of the systems B1 and B2 as well as different fitting approaches for B2.

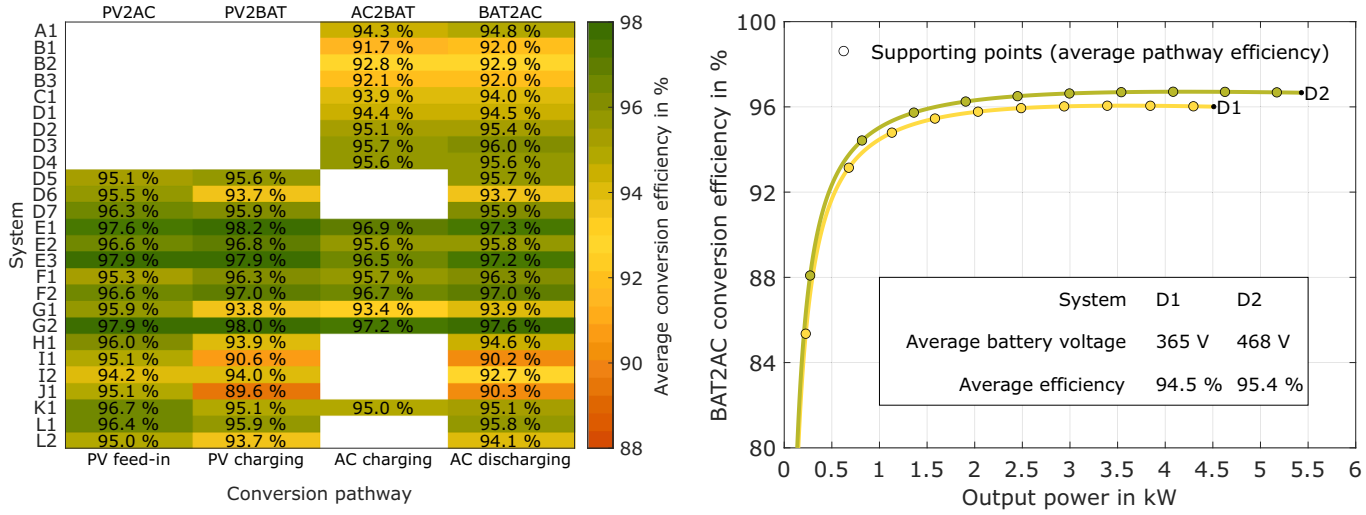

Fig. 12. The average efficiency of the different conversion pathways (left) of the AC-coupled systems A1 to D4 and the DC-coupled systems D5 to L2. BAT2AC pathway efficiency and supporting points (right) to determine the average efficiency of the AC-coupled systems D1 and D2.

of the different conversion pathways for the 26 analyzed systems. As already analyzed before, a small difference between the nominal PV input voltage and the DC link voltage of the inverter has a positive effect on the PV2AC conversion efficiencies. The average is 96.1 % and the median value is 96.0 %. The PV battery charging efficiencies of the DC-coupled systems (PV2BAT) are mostly in the same range. However, the difference between the maximum (98.0 %) and minimum (89.6 %) average PV2BAT path efficiency is significantly higher than for the PV feed-in (PV2AC). Therefore, the mean (95.1 %) and the median value (95.6 %) also differ by 0.5 percentage points. As the shape of the efficiency curves already indicated, the average AC charging and AC discharging conversion efficiencies of the AC-coupled storage systems differ only slightly from each other. For the DC-coupled systems of manufacturer E, the average AC charging efficiencies are between 1.2 and 1.4 percentage points below the average PV charging efficiency. However, in most cases, they are still higher than the average charging efficiency of the AC-coupled systems. System G2 achieves the highest efficiencies in all energy conversion paths, with values above 97.2 %. In discharge mode, it achieves an average conversion efficiency of 97.6 %. In contrast, the average AC discharge efficiency of systems I1 and J1 is more than 7 percentage points lower.

When interpreting the average path efficiencies, it is important to consider that, for example, the load-dependent activation of individual components has an effect on the parameter. Furthermore, the average conversion efficiencies are influenced by the nominal power of the individual systems. Fig. 12 (right) illustrates the dependence of the BAT2AC conversion efficiencies on the output power for the AC-coupled systems D1 and D2. Moreover, the figure shows the 10 equally spaced supporting points that are used to determine the average path efficiency. The two systems differ only in the number of battery modules connected in series. The DC discharge current is therefore identical for both systems and limited to 13 A. Due to the approximately 100 V higher battery voltage of system D2, the nominal AC discharge power increases from 3.2 kW (D1) to 4.5 kW (D2). Since the 10 supporting points are dependent on the nominal power, they increasingly shift towards higher power values in the case of higher nominal power levels. This results in significantly improved efficiencies, especially at the supporting points in the lower power range. In the medium and upper power range, however, the influence of the battery voltage on the efficiencies is predominant. The difference in efficiency between the systems D1 and D2 varies by only 0.5 to 0.7 percentage points at a discharge power of 1 kW to 4 kW. Nevertheless, the mean BAT2AC conversion efficiencies of the two systems differ by almost 1 percentage point. Thus, the average conversion efficiencies are not only influenced by the battery voltage, but also by the level of the nominal power of the different systems.

Table VI shows the median and mean values of the different average conversion pathways efficiencies.

2.5. Control deviation

In addition to the system losses due to power limitations or energy conversion, different control-related losses occur in PV battery systems. The MPP tracker is not always able to set the optimal operating point of the PV generator. Furthermore, additional restrictions such as minimum charging and discharging power thresholds, recharging hysteresis or an end-of-charge phase with reduced charging power are partially implemented in the control of battery systems [22]. However, dynamic and stationary control deviations are mainly responsible for the control losses [22] and will be analyzed in the following.

2.5.1. Dynamic control deviation

The battery charge or discharge power is adjusted with respect to the active power flows measured at the point of grid connection. These flows are affected by the on-site generation and load demand [102]. The main reason for abrupt changes in PV output are shadows caused by passing clouds [103]. In addition, the switching of electrical appliances causes high peaks and steep ramps in the demand curve [104]. The power of the PV system as well as the duration of a demand peak can fluctuate rapidly on a time scale ranging from several minutes to a few seconds [105]. Since the objective of a PV battery system is to minimize energy exchange with the grid, the battery controller must be able to react to these short-term changes. To ensure control stability and due to the general fact that information acquisition and processing procedures commonly have an inherent time delay, the battery power control is subject to the response time and a damped adjustment of the battery power [102]. To measure the so-called dead and settling time, a step response test is defined in the efficiency guideline [72]. In addition to a step profile with

Table VI
Median and mean values of the average conversion efficiencies.

	Median	Mean
battery efficiency in %	96.1	96.0
PV2AC-conversion efficiency in %	96.0	96.1
PV2BAT-conversion efficiency in %	95.6	95.1
AC2BAT-conversion efficiency in %	95.1	94.9
BAT2AC-conversion efficiency in %	95.0	94.6

fluctuating loads, a constant power generation is specified in the laboratory, see Fig. 13 (top left). Thus, the 14 different power steps result in an alternating charging and discharging behavior of the analyzed device during the laboratory test. The holding time of the individual steps is set to twice the response time identified in a preliminary step response test, but at least to 10 s. Since the dynamic control deviations can vary depending on the instant in time the load step is applied and the magnitude of the load step [43,71], as well as to exclude outliers and other statistical errors, the fluctuating step profile is repeated ten times. Finally, the system parameters are calculated from the mean values of the individual iterations. Fig. 13 (top left) additionally shows the resulting grid power, which, depending on the load power step, results in a grid feed-in or a grid power supply.

To further analyze how the dynamic control deviation of a system affects the grid exchange power, Fig. 13 (top right) shows the 13th step (240 s to 260 s) of the first iteration displaying system D3 as an example. Since the load power is below the PV power, the system is in discharge mode. Here, the dynamic control deviations have different effects on the resulting energy flows. After the sudden increase in the residual power (PV power minus load), the grid must supply the raised demand until the transient process is completed. The acquisition and processing of the measured data results in a time delay of 0.4 s between the load change and the start of the power adjustment of the battery system. Nevertheless, the resulting settling time of system D3, which is required to compensate for the power change, is significantly longer. The length of the transient response corresponds to the time between the load change and the time it takes for the battery power to reach the tolerance band (± 5 %) of the new stationary battery power without leaving it again. System D3 reaches the new set point on average after an oscillating transient response (second-order time delay) of 2.7 s. In contrast, a different behavior can be observed with decreasing power demand. Due to the delay, the battery system now feeds part of its power output into the grid.

Usually, the response time to change the PV power is identical to the dead time for load changes. However, manufacturer E states that its systems can react faster to changes in PV power. Unfortunately, this cannot be verified yet with the current test conditions of the efficiency guideline.

Munzke et al. and Weniger et al. were able to show that the losses in real operation due to the dynamic control deviations are primarily caused by the delayed reaction to load changes [69,102]. The latter publication also reveals that the slower the battery control, the greater the undesired exchange of energy with the grid.

Fig. 13 (bottom) shows the average dead and settling times of the analyzed systems. During the tests, dead times of less than 0.2 s (G1, G2, I1, I2) up to 2.8 s (E2) were determined. While digital power sensors measure the voltage and current at the point of grid connection in most of the systems investigated, in the systems of manufacturer G and in devices B1 and B3 only the current measurement is located at the point of grid connection, while the voltage is measured in the system. The differences in the dead time can be related, among other things, to the different measurement value acquisition and data transfer intervals. The higher dead time of B2 compared to the other systems of manufacturer B could result from to the different power sensor that has to be additionally installed when cascading.

After a change in the electrical load, it takes an average of 1.1 s before the power adjustment of the storage system begins. Within this period, the whole settling process of systems G1 and G2 is already completed. Their settling time is lower than the dead time of 13 of the 24 other systems evaluated. The high settling time of the systems E1 (14.2 s) and K1 (13.8 s) is partly due to an oscillating behavior of the battery power which is observed in these systems after the first entry into the tolerance range around the new set point value. However, with an oscillating transient response (D1 to D7), similar settling times can be achieved as with a damped transient response like a first-order time delay (e.g. I1 to I2). While the mean settling time is 5.6 s, the median is

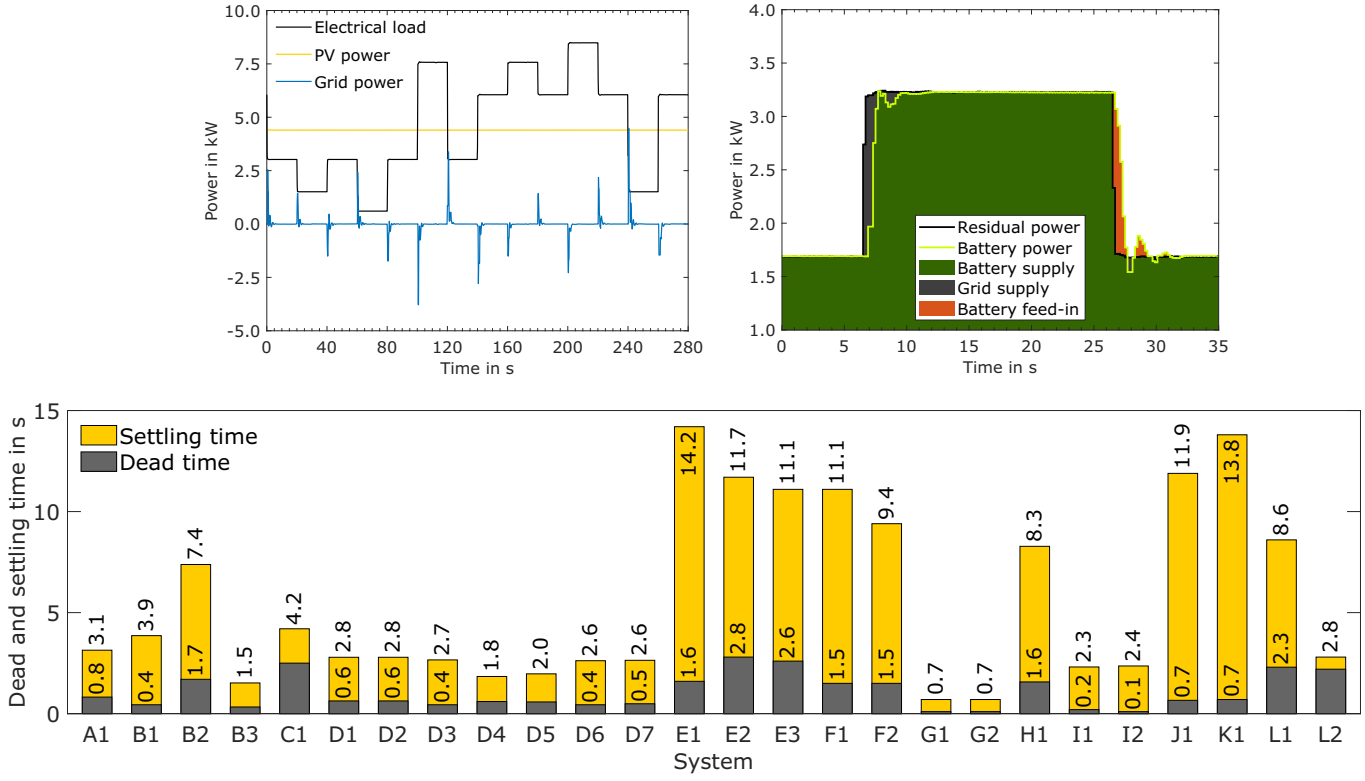

Fig. 13. Step profile (top left) to characterize dynamic control deviation (example: system D3). Step response behavior and resulting power flows (top right) during the test to determine the dynamic control deviation in the discharge mode (example: system D3). Average dead and settling time (bottom) of the analyzed systems.

3.0 s.

2.5.2. Stationary control deviation

Furthermore, control deviations occur during operation even at times with constant PV power output or constant electrical load. Ideally, a PV battery system can regulate the power at the point of grid connection to zero in these stationary conditions by adjusting the battery power. In real operation, however, differences between the set point and the actual values of the battery power occur [43,71] and power is fed into or drawn from the grid. This can be attributed, for example, to measurement inaccuracies or to set point deviations. The latter is implemented by some manufacturers to prevent battery discharge into the grid, which can quickly occur with a stationary control deviation close to 0 W due to frequent load changes [45].

The stationary control deviations are also measured using the step profile, see Fig. 14 (top). However, for this test 2 iterations are usually sufficient. Each stage is longer with a total holding time of 160 s. The integration and averaging interval is 80 s and starts 60 s after the load change, so that the transient process is already finished. In total, the efficiency guideline defines 6 load states, 3 each for charging (state L1 to L3) and discharging (state E1 to E3), where the load level is fixed and identical (e.g. state E3: steps 8, 10, 12, 14) [72]. For the evaluation, the measured values of the grid supply power and the grid feed-in power are first averaged over the steps assigned to the load state and the 2 iterations. Subsequently, the averaging is carried out over the 3 charging or discharging states. Grid feed-in occurs at the points where, for example, the battery cannot fully absorb the available power during charging. In contrast, the energy supply from the grid increases when the battery charge power exceeds the set point. In the case of discharging, it is the other way around. If oscillating behavior occurs under stationary conditions, both energy flows appear.

Fig. 14 shows the determined stationary control deviations for the charging (middle) and discharging (bottom) cases for all analyzed systems. With 16 out of 26 systems, the majority show low stationary control deviations of less than 10 W in both operating states. Eleven of these systems exchange on average less than 5 W with the grid. As the graphs in Fig. 14 (top) and (middle) show, system D3 primarily draws energy from the grid in the charging process (apart from the load state

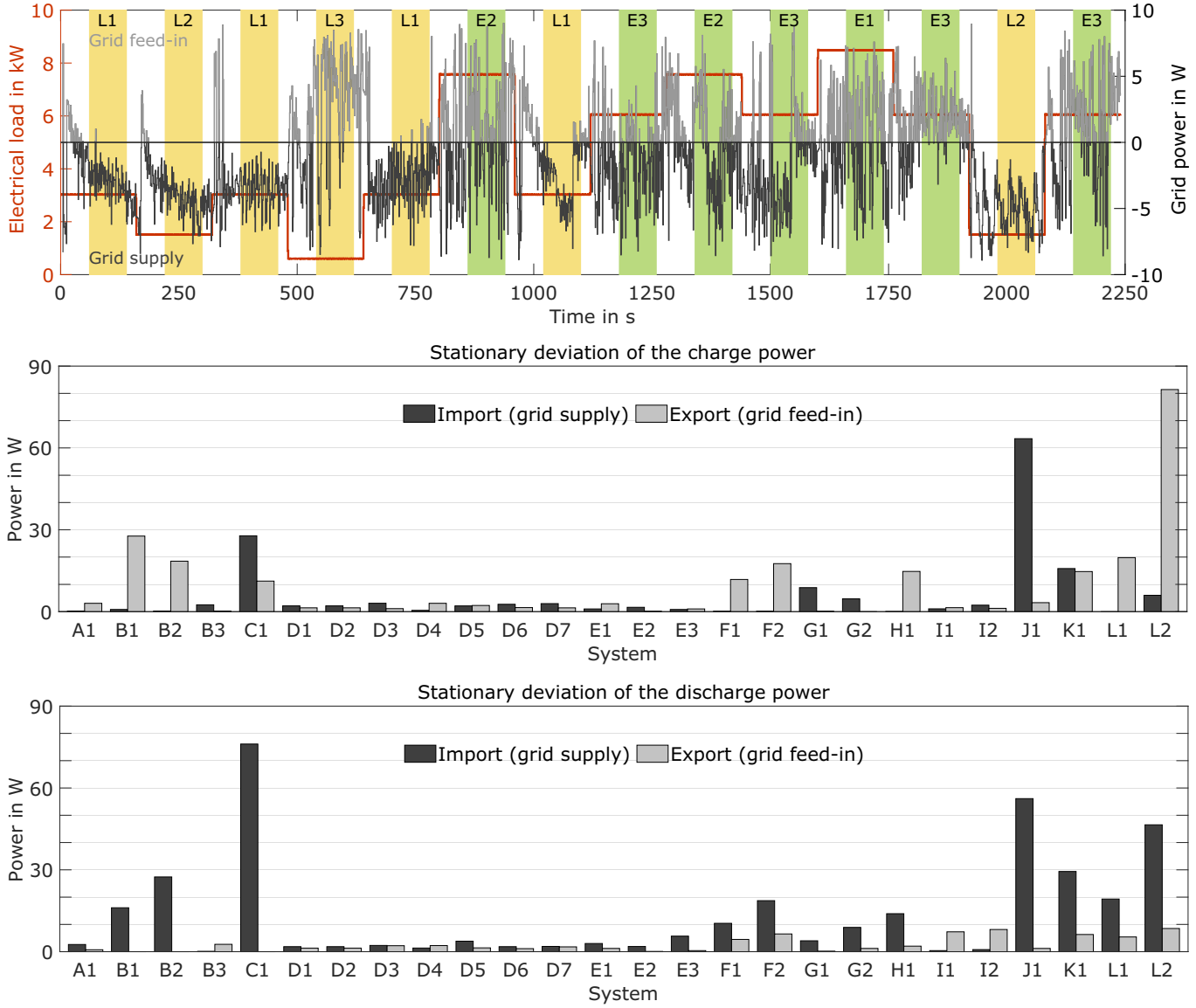

Fig. 14. Measured values of the stationary control deviations of the system D3 for the first iteration and integration intervals of the different load states indicated by the green and yellow color (top). Average stationary control deviation of the charge (middle) and discharge power (bottom) of the analyzed systems. (For interpretation of the references to color in this figure legend, the reader is referred to the web version of this article.)

L3). In system J1, the charging power exceeds the available surplus PV power not only by 3 W (D3), but by an average of 63 W, which is covered by the grid. In contrast, in the systems of manufacturers F and L, as well as in systems B1, B2 and H1, an average feed-in power between 12 W and 81 W occurs in charging mode. Control-related power excesses during charging always lead to an undesired increase in energy exchange with the grid. Power deficits that lead to grid feed-in can have a negative impact if the battery does not become full. During discharge mode, systems B1, B2, C1, and J1 to L2 in particular do not provide sufficient power. To cover the electrical load, an additional 16 W to 76 W must be supplied by the grid. These power deficits can have a negative impact if the battery is not completely discharged until the next charging period. In contrast, unintentional battery feed-in to the grid occur more frequently with the systems of manufacturer I. The stationary control deviations of system B3 were only recorded in the laboratory with a single-phase electrical load. System B3 measures the currents via current transformers at the point of common coupling. However, this single-phase system only records the voltage of the phase to which it is connected. As a result due to line impedances and resulting losses, the control deviations of system B3 can be significantly higher in real operation in the event of voltage unbalances between the three phases [34].

2.6. Power consumption in standby mode

In addition to the system losses during charging and discharging, the power consumption of the individual components in standby mode leads to further losses in storage systems. A primary distinction can be made between the standby consumption in a fully charged and fully discharged state. Depending on the system sizing, a PV storage system remains discharged between 2000 h and 4000 h per year. In contrast, the system spends only 1000 h to 2000 h per year in a fully charged state [22]. Furthermore, peripheral components such as current sensors or energy meters must be supplied throughout the year. Depending on the level of power consumption, standby losses can have a decisive influence on the level of total losses of a PV battery system [23,30,34]. Here, the standby power in the discharged state has a greater influence than the standby power in the fully charged state due to the longer dwell time in the respective state. To measure the standby power consumption, the systems are fully charged or discharged in the test laboratory, which causes them to switch automatically into standby mode. When determining the power consumption in the discharged state, only a load for 25 % of the nominal discharged power is applied. In contrast, when measuring the power consumption at the maximum SOC, according to the efficiency guideline 75 % of the PV power must also be present to keep the system in a fully charged state. To determine the power consumption of the peripheral components, the PV simulator and the electrical load are deactivated, and the battery is fully discharged.

After the system reached a stable state, the relevant AC and DC power values are measured over a period of 1 min. This data is then recorded for a duration of up to 3 h. If there is a significant and permanent change in consumption within this time, a new measurement is carried out for 1 min after the change has occurred [72].

Fig. 15 shows an example of the measured values of the AC and DC power consumption of system B3 after reaching the discharged state. Already 1 min after the battery finished discharging, the system reduces its AC power consumption from 11 W to 3 W. After a total of 6 min, the system reaches its final standby mode and stops drawing DC power from the battery. At the same time, the AC power consumption from the grid is reduced from 3 W to 2 W. The first mode is often called idle mode, in which the system must be ready to react immediately to load changes. The last mode, on contrary, is also called sleep mode, as the system needs more time to be able to operate in regular mode again [43]. In the fully charged state, a comparable behavior can be observed for system B3.

The laboratory measurement results show that various

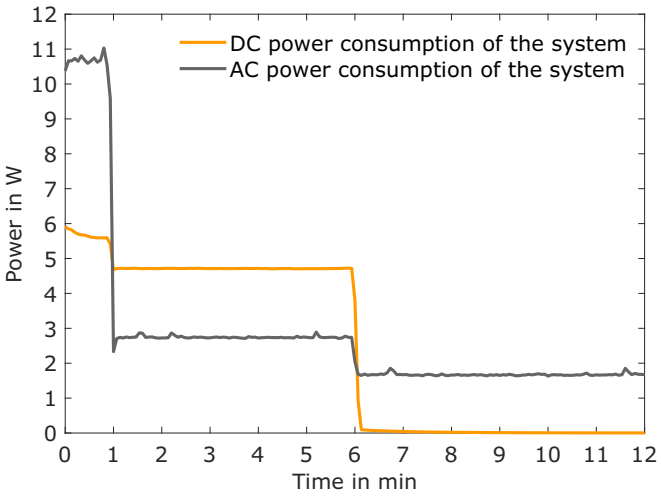

Fig. 15. Measurements during the test to determine the standby consumption of a battery system in the discharged state (example: system B3).

manufacturers have implemented several standby modes (e.g. A1, B3, D3, E1-E3, and I1). In the systems of manufacturer E as well as in A1 and I1, the additional standby mode reduces the power consumption in the discharged state by a factor of about 3 to around 10 W. However, the entry time into the mode after the battery has finished discharging varies between 5 min and 10 min. Since storage systems usually remain in the reduced power mode for the longest time, the standby consumption is specified for this state.

Fig. 16 (top) shows a comparison between the standby power consumption of the investigated systems when the battery is discharged. Most of the AC- and DC-coupled systems tested draw power mainly on the AC side to supply the control electronics, the communication module and other system components. The different standby powers of the identical hybrid inverters F2 (13 W) and H1 (29 W) are due to different firmware versions. In some systems, the inverter is additionally or almost entirely powered on the DC side by the battery. Only the systems G1 and G2 draw power exclusively from the battery. During real operation, however, their batteries must be protected from deep discharge by being regularly recharged with electricity from the grid, especially during the winter period. In these two systems, the AC sensor consumption is already included in their power consumption. In contrast, system I1 supplies itself via a separate power supply unit. Its power consumption is therefore assigned to the AC sensor consumption. System L2 shows another different operating behavior, which remains unchanged even at the end of the test after more than 4.5 h. When discharged, it draws 101 W from the battery and delivers 32 W directly to the AC side to further cover the load. Thus, the hybrid inverter does not require the entire DC power provided by the battery. This results in a standby power consumption in the discharged mode of 71 W. In contrast, the lowest standby consumption is only 2 W (B1 and B3). On average, the power consumption is 18 W and the median is even lower at 12 W.

In the fully charged state, the power consumption of the analyzed systems also varies greatly between 1 W and 45 W, see Fig. 16 (bottom). However, 13 of the 26 systems draw less than 4 W. Accordingly, the mean (9 W) and median (5 W) values are lower compared to the discharged state. In this case, the AC power consumption of the AC-coupled systems is covered by the PV system and reduces the energy fed into the grid. The battery is discharged in half of the systems to supply the inverters. Manufacturer E was able to eliminate the DC power consumption (44 W) of the hybrid inverter integrated into the systems E1 and E3 via a software update. In the DC-coupled systems D6, E2 to F2, H1, J1, L1, and L2 only the consumption of the AC power sensor occurs in the fully charged state. In contrast, system I1 discharges the battery with 33

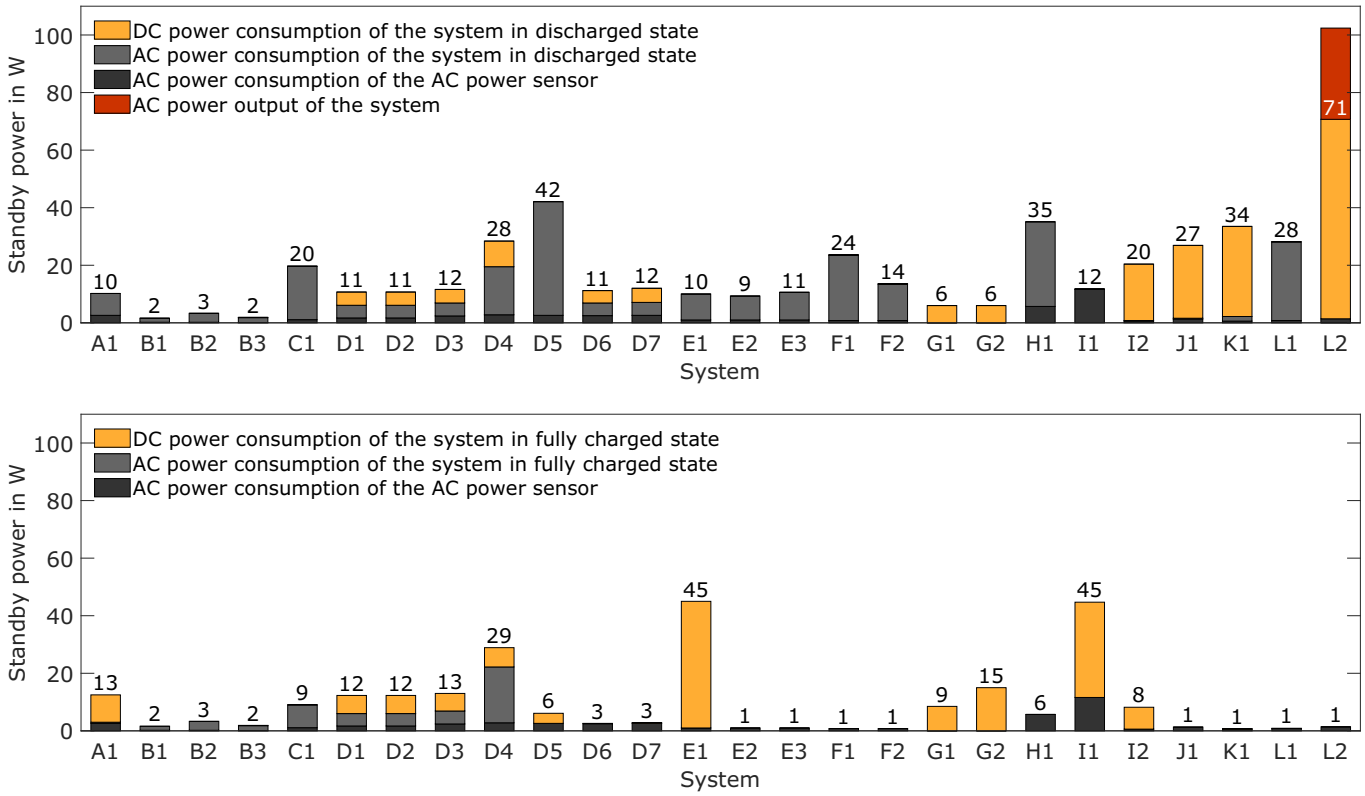

Fig. 16. Composition of the standby power consumption of the analyzed systems in a fully discharged state (top) and a fully charged state (bottom).

W after the charging process has been terminated. Together with the AC power consumption of the separate power supply unit, this results in a total standby consumption of 45 W.

The highest permanently applied power consumption of the peripheral components is found in the systems H1 and I1 with 6 W and 12 W. No direct relationship between the system size and the power consumption in the standby mode can be identified.

Table VIII in the appendix provides an overview of the most important so-called application-independent performance characteristics of the systems investigated.

3. Discussion

The following section provides an overview of influencing factors that should generally be considered when interpreting measured values that have been recorded according to the efficiency guideline. In addition, further characteristics are listed which influence the system efficiency of PV home storage systems in operation.

3.1. Test conditions of the efficiency guideline

The efficiency guideline defines uniform measurement methods for determining the efficiency, standby consumption, and controller effectiveness of stationary battery storage systems. Büchle et al. and Kulkarni et al. were able to show a largely satisfactory repeatability of the measurement results with their comparison of the corresponding measured values collected in four different test institutes [63,74]. Nevertheless, the data quality varies depending on the test stand. Differences can occur, for example, due to the measurement equipment and their measuring accuracy or due to different evaluation methods or algorithms as well as different interpretations of the evaluation specifications [63,75]. The authors therefore recommend clarifying, supplementing and specifying various formulations. At the same time, the test results should be regularly compared with other testing institutes. Moreover, they identified potential for improvement in some existing processes and developed new approaches.

In order to keep the costs of the laboratory tests low, a rather wide range of the permissible ambient temperature of 20 °C to 30 °C was specified in the efficiency guideline [72]. However, the electrical properties and thus the conversion efficiencies of the battery and power electronic system components are influenced by the ambient temperature [106,107]. For example, battery efficiency increases with temperature, mainly due to reduced internal cell resistance [108]. For more consistent results, Büchle et al. recommend further restricting the temperature range for determining battery efficiencies and capacities [74].

When comparing the power dependence of the battery efficiency of all analyzed systems, it was found that the battery efficiency determined at the medium battery power (50 %) deviated on average by only −0.22 percentage points from the mean value of the three measurement points 25 %, 50 %, and 100 %. The range varies between −0.51 and + 0.19 percentage points. However, for 23 of the 25 systems, the determined battery efficiency is below the values shown in Fig. 6. The deviations in battery capacity range from −0.24 kWh to +0.46 kWh. However, only in 3 systems it is above ±0.1 kWh. If battery capacity and efficiency are only recorded at medium battery power, the duration of the battery efficiency test can be reduced by at least a factor of 3. RTE measurements account for approximately 30 % of the total installation, testing and evaluation time. At the same time, the costs and effort for the manufacturers decrease.

According to the efficiency guideline, the efficiency curves of the individual conversion paths are determined by reducing the power in certain steps starting from the nominal power. However, it should be taken into account that the control and therefore the battery power of individual systems react differently accurately to decreasing or increasing power [45]. In addition, the specified test sequence affects the operating temperature of the semiconductors and thus the conversion efficiency [109].

As mentioned previously, the PV feed-in (PV2AC) and PV battery

charging (PV2BAT) efficiency curves of the DC-coupled systems are compared at the nominal PV input voltage defined by the manufacturer. However, they vary depending on the system. In addition, in real operation, the resulting PV generator voltage is largely determined by the nominal power and the electrical circuitry of the PV generator. For example, the nominal voltage is often significantly higher than the actual input voltage when the PV generator is split between different inputs of the inverter. As a result, the conversion losses in real operation may be higher than those determined in the laboratory test at nominal input voltage. Therefore, according to the efficiency guideline, PV2AC and PV2BAT efficiencies are also determined at the minimum and maximum MPP voltage specified by the manufacturer. However, the analysis of the laboratory reports has shown that at these voltages the conversion efficiencies for some systems cannot be recorded at all power levels. This is due, for example, to current limitations or inaccurate MPP tracking for small PV currents. In addition, undesired power flows that do not belong to the measured path (e.g. battery charging when measuring PV2AC) occur more often at the voltage limits.

Furthermore, the conversion efficiency of battery charging (PV2BAT and AC2BAT) and battery discharging (BAT2AC) was determined at medium battery voltage. Fig. 8 (bottom) shows that the difference between the maximum and minimum battery voltage can vary by several hundred volts for high voltage systems. Consequently, at the voltage limits, the conversion efficiency of the power electronics can deviate significantly from the conversion efficiencies determined at the medium battery voltage [69].

Moreover, it should be noted that combined power flows (PV2AC and BAT2AC or PV2AC and PV2BAT) occur in DC-coupled storage systems in real-life applications [23]. These power flows cannot be accurately represented via individual power loss analyses according to the efficiency guideline. A simple superposition of the power losses leads to an overestimation of the losses due to the double-counting of the idle losses [110]. This should be considered in simulation analyses.

Regarding the control effectiveness of the systems, it should be noted that the test reports only provide the average stationary and dynamic control deviations. However, a power dependency can occur [102].

Moreover, a method should be developed to determine the dynamic control deviations of DC-coupled PV battery systems during changes in PV power. These may differ from deviations during load changes. During operation, however, the stationary control deviations can also show an inconsistent, strongly power-dependent control behavior [71]. Kulkarni et al. have also shown that the current test method of the stationary control deviation procedure has limited reproducibility of the results. Therefore, they have proposed an alternative profile with a reduced number, height and sequence of steps [63].

In addition, individual test reports indicate that during the battery test it was not clear for all iterations whether the criteria for determining the end of charge had been reached and whether the battery was fully charged. Therefore, the tests were repeated. These criteria can also become problematic when measuring, for example, high-temperature (sodium-nickel-chloride) batteries, where the battery charge can be very protracted without falling below the limit value. Furthermore, when the second criterion is applied (the battery charging power has fallen below 3 % of the charging power over 1 h), a lower efficiency is often measured. For these reasons, it seems useful to identify further criteria for determining the fully charged state.

Finally, it should be noted that, according to the efficiency guideline, the system must be measured over a period of 3 h to correctly record the standby power in the fully charged and discharged state. However, it can often already be identified in preliminary measurements that no changes will occur during this period. A clear definition can therefore reduce the total measurement period.

3.2. Other observed factors influencing the operating behavior

In addition, there are certain effects during the operation of the PV home storage systems that are not covered by the measurements according to the efficiency guideline. Due to production tolerances, different operating conditions, or varying temperature distribution in the battery pack, there are differences in the capacity of the individual battery cells connected in series with increasing operating time [111]. To extend the lifetime of the battery, the battery cells are equalized from time to time to keep the difference between the cells as small as possible [111,112].

In addition, especially during the winter months, as soon as the SOC falls below a specified threshold value, grid recharging is carried out to protect the battery from deep discharge. For the same reason, one manufacturer reduces the usable DOD during this period [113]. Furthermore, calibration charges can be identified when analyzing operational data. These usually serve the purpose of ensuring correct SOC indications or determining the reduced battery capacity due to aging [112]. Apart from battery recharging, increased ambient temperatures at the installation site may result in a more frequent operation of a fan, whose power consumption influences the conversion efficiency.

Moreover, it should be noted that some systems have an integrated threshold for activating the charge or discharge mode. Thus, for example, discharging is only possible when the load is above a certain level [114]. This can result in higher discharge efficiency, but depending on the battery capacity and the load power, the system may not be fully discharged during nighttime.

Integrated operating strategies can have a positive impact on the system efficiency and the lifetime of PV home storage systems during their use. A forecast-based operating strategy shifts the charging of the battery storage system to periods of high PV power output, which reduces the curtailment losses due to a potentially required limit of the feed-in power [115]. At the same time, delayed battery charging reduces the dwell time of the battery in the maximum SOC. This has a positive impact on the battery life of lithium-ion batteries, as it slows down calendar aging in particular [32,85,116]. The aging behavior of individual residential battery systems can be found in the ITP Renewables study [67]. In addition to the reduced usable battery capacity, battery efficiency is expected over the life of the battery due to increased battery impedance [97]. Furthermore, efficiency-optimized system control can reduce conversion losses by avoiding the operation of power electronic components in the partial load range [117].

4. Conclusion and outlook

This paper compares the performance characteristics of 26 commercially available state-of-the-art residential PV battery storage systems. They were measured according to the efficiency guideline for PV storage systems. The presented performance characteristics can be attributed to the following loss categories: sizing, conversion, control, and standby losses. Besides the nominal power and the usable battery capacity, the efficiency of the inverter and the power conversion system were analyzed. Furthermore, the paper compares the dead and settling time and the stationary control deviations as well as the AC, DC, and peripheral power consumption in a fully charged and discharged mode. At the same time, the test procedure for determining the various properties is described in detail using real measured values.

The usable battery capacity varies between 5.8 kWh and 16.7 kWh. The evaluation shows that the usable capacity measured and specified by the manufacturer in the data sheet deviates by up to 19 %. The conversion efficiency of the different systems also differs considerably in some cases. For example, the battery efficiency of the investigated systems varies by up to 10 percentage points, ranging from 88 % to 98 %. DC-coupled PV storage systems are often advertised with inherently higher efficiencies compared to AC systems. However, high efficiencies can also be found in AC systems, while low efficiencies do also occur in DC systems. A comparison of the minimum and maximum values of the different path efficiencies shows that in some cases there are differences between the hybrid inverters of up to 8 percentage points occur. DC

systems can exploit their efficiency advantages when they are coupled with high voltage batteries. While the most efficient systems achieve average path efficiencies of more than 97 %, the values of the less efficient systems are only 90 %. Besides the high voltage, the excellent conversion efficiency is also due to the use of silicon carbide semiconductors.

In addition, the analysis shows that the best residential battery systems can nowadays fully compensate for power steps within just 700 milliseconds. In contrast, the results show that other systems need up to 14 s to compensate for the new power demand. At the same time, some systems regulate the power at the point of grid connection nearly to zero, while others exceed or fall short of the new target value by up to 80 W. These differences are related to the different fast and accurate measurement value acquisition and data processing of the current sensors or energy meters.

Furthermore, significant differences in standby power consumption can be identified. In addition to the use of power-efficient components, some systems switch to a state with low energy consumption shortly after entering standby mode. While several systems draw less than 3 W, the constant power consumption of one system is over 70 W, when fully discharged.

A comparison with the previous publications by Munzke [23,32], Niedermeyer [45] and Kairies [71] shows that, on average, numerous performance characteristics of the systems have improved, despite higher power and usable battery capacities. In addition to higher battery efficiencies, higher conversion efficiencies can be identified for PV feed-in, battery charging and discharging. Furthermore, several manufacturers seem to be increasingly addressing the issues of high standby power consumption and high dead and settling times.

However, the range of performance characteristics shows that there is still significant potential for optimization in residential PV battery systems, especially in terms of conversion efficiency and standby power consumption. High system losses have an impact not only on the economical but also on the ecological efficiency of the overall system. In addition, the described parameters can be used to parameterize more detailed simulation models to obtain more accurate results. The consideration of all system losses can thus have an impact on the system dimensioning and decisive economic parameters can be estimated in more detail in advance. However, it should be noted, that not all losses that occur during the operation of the PV home storage systems can be identified by the test procedure according to the efficiency guideline. These include, for example, balancing losses, calibration charges, or grid recharging to protect the battery from deep discharge. Furthermore, additional losses such as energy management losses as well as aging aspects of PV battery storage systems in residential buildings need to be analyzed in further studies.

CRediT authorship contribution statement

Nico Orth: Conceptualization, Methodology, Software, Formal analysis, Investigation, Data curation, Writing – original draft, Visualization. **Nina Munzke:** Conceptualization, Investigation, Writing – review & editing, Funding acquisition. **Johannes Weniger:** Conceptualization, Investigation, Visualization, Methodology, Writing – review & editing, Funding acquisition. **Christian Messner:** Writing – review & editing. **Robert Schreier:** Writing – review & editing. **Michael Mast:** Writing – review & editing. **Lucas Meissner:** Writing – review & editing. **Volker Quaschning:** Funding acquisition, Resources, Project administration, Writing – review & editing, Supervision.

Declaration of competing interest

The authors declare that they have no known competing financial interests or personal relationships that could have appeared to influence the work reported in this paper.

Data availability

The authors do not have permission to share data.

Acknowledgements

The research project “Perform“(Grant No. 03EI3039A) is funded by the Federal Ministry for Economic Affairs and Climate Action (BMWK). The authors thank the project management organization Jülich (PtJ) and the BMWK. The work at KIT additionally contributes to the research performed at (KIT-BATEC) KIT Battery Technology Center and CELEST (Center for Electrochemical Energy Storage Ulm-Karlsruhe).

Appendix A

Table VII
Different key indicators of the analyzed systems.

System	Topology	Nominal PV input power in kW	Nominal charge power in kW	Nominal dis-charge power in kW	Usable battery capacity in kWh	Normalized power in kW/kWh
A1	AC	–	4.4	4.8	15.7	0.30
B1	AC	–	2.3	2.5	5.8	0.43
B2	AC	–	4.5	5.0	11.5	0.43
B3	AC	–	2.3	2.5	5.8	0.43
C1	AC	–	4.3	4.7	10.0	0.47
D1	AC	–	4.9	4.7	–	–
D2	AC	–	5.4	5.6	10.5	0.54
D3	AC	–	9.4	10.4	12.1	0.85
D4	AC	–	4.1	4.0	7.4	0.54
D5	DC	4.7	4.1	3.9	7.4	0.53
D6	DC	5.6	4.2	4.0	7.1	0.56
D7	DC	10.3	6.6	6.6	12.3	0.53
E1	DC	10.2	9.7	10.1	9.7	1.04
E2	DC	6.3	6.0	6.0	7.4	0.81
E3	DC	10.4	9.4	9.1	9.9	0.92
F1	DC	5.2	5.0	5.1	7.3	0.69
F2	DC	10.4	9.7	10.2	12.2	0.83
G1	DC	6.2	6.6	6.1	7.0	0.87
G2	DC	10.4	12.4	10.4	10.6	0.98
H1	DC	10.3	8.2	7.8	16.2	0.48
I1	DC	12.7	4.4	4.7	11.1	0.42

(*continued on next page*)

Table VII (*continued*)

System	Topology	Nominal PV input power in kW	Nominal charge power in kW	Nominal dis-charge power in kW	Usable battery capacity in kWh	Normalized power in kW/kWh
I2	DC	12.6	6.3	6.3	11.7	0.54
J1	DC	10.3	5.1	4.9	7.5	0.65
K1	DC	11.4	9,5	9.1	16.7	0.55
L1	DC	10.3	7,5	7.0	13.5	0.52
L2	DC	11.5	7.4	7.3	13.4	0.54

Table VIII
Application-independent characteristics according to the [72]. The listed vales are average values.

	A1	B1	B2	B3	C1	D1	D2	D3	D4	D5	D6	D7	E1
PV2AC-conversion efficiency in %	–	–	–	–	–	–	–	–	–	95.1	95.5	96.3	97.6
PV2BAT-conversion efficiency in %	–	–	–	–	–	–	–	–	–	95.6	93.7	95.9	98.2
AC2BAT-conversion efficiency in %	94.3	91.7	92.8	92.1	93.9	94.4	95.1	95.7	95.6	–	–	–	96.9
BAT2AC-conversion efficiency in %	94.8	92.0	92.9	92.0	94.0	94.5	95.4	96.0	95.6	95.7	93.7	95.9	97.3
battery efficiency in %	95.1	98.0	98.0	97.8	95.5	–	95.3	96.4	96.0	96.0	96.2	96.5	96.1
Settling time in s	3.1	3.9	7.4	1.5	4.2	2.8	2.8	2.7	1.8	2.0	2.6	2.6	14.2
Power consumption in standby mode (discharged state) in W	10	2	3	3	20	11	11	12	28	42	11	12	10
	E2	E3	F1	F2	G1	G2	H1	I1	I2	J1	K1	L1	L2
PV2AC-conversion efficiency in %	96.6	97.9	95.3	96.6	95.9	97.9	96.0	95.1	94.2	95.1	96.7	96.4	95.0
PV2BAT-conversion efficiency in %	96.8	97.9	96.3	97.0	93.8	98.0	92.9	90.6	94.0	89.6	95.1	95.9	93.7
AC2BAT-conversion efficiency in %	95.6	96.5	95.7	96.7	93.4	97.2	–	–	–	–	95.0	–	–
BAT2AC-conversion efficiency in %	95.8	97.2	96.3	97.0	93.9	97.6	94.6	90.2	92.7	90.3	95.1	95.8	94.1
Battery efficiency in %	96.9	96.9	97.0	97.0	95.2	95.6	95.5	97.4	96.7	87.9	95.8	95.6	95.4
Settling time in s	11.7	11.1	11.1	9.4	0.7	0.7	8.3	2.3	2.4	11.9	13.8	8.6	2.8
Power consumption in standby mode (discharged state) in W	9	11	24	14	6	6	35	12	20	27	34	28	71

Table IX
Median and mean values of the application-independent characteristics shown in Table VIII. The values of the average conversion efficiencies can be found in Table VI.

	Median	Mean
Settling time in s	3.0	5.6
Power consumption in standby mode (discharged state) in W	12.0	18.2

References

[1] S. Comello, S. Reichelstein, The emergence of cost effective battery storage, Nat. Commun. 10 (2019) 2038, https://doi.org/10.1038/s41467-019-09988-z.

[2] European Commission, Joint Research Centre., Li-ion batteries for mobility and stationary storage applications: scenarios for costs and market growth, Publications Office, LU, 2018 (accessed July 22, 2022), https://data.europa.eu/doi/10.2760/87175.

[3] S.B. Wali, M.A. Hannan, P.J. Ker, M.A. Rahman, M. Mansor, K.M. Muttaqi, T.M. I. Mahlia, R.A. Begum, Grid-connected lithium-ion battery energy storage system: a bibliometric analysis for emerging future directions, J. Clean. Prod. 334 (2022), 130272, https://doi.org/10.1016/j.jclepro.2021.130272.

[4] The International Renewable Energy Agency (IRENA), Electricity Storage And Renewables: Costs and Markets to 2030, The International Renewable Energy Agency (IRENA), Abu Dhabi, United Arab Emirates, 2017.

[5] U.S. Energy Information Administration, EIA - Electricity: Analysis & Projections - EIA-860, Year 2020. https://www.eia.gov/electricity/data/eia860/, 2022. Niestetal.

[6] SolarPower Europe, European Market Outlook for Residential Battery Storage 2021-2025, 2021.

[7] B.-K. Jo, S. Jung, G. Jang, Feasibility analysis of behind-the-meter energy storage system according to public policy on an electricity charge discount program, Sustainability. 11 (2019) 186, https://doi.org/10.3390/su11010186.

[8] BloombergNEF, Global Energy Storage Outlook: Presentation for Macquarie Group, 2021.

[9] J. Figgener, P. Stenzel, K.-P. Kairies, J. Linßen, D. Haberschusz, O. Wessels, G. Angenendt, M. Robinius, D. Stolten, D.U. Sauer, The development of stationary battery storage systems in Germany – a market review, J. Energy Storage 29 (2020), 101153, https://doi.org/10.1016/j.est.2019.101153.

[10] International Energy Agency (IEA), IEA: Energy Storage. https://www.iea.org/reports/energy-storage, 2022 (accessed July 26, 2022).

[11] L. Mauler, F. Duffner, W.G. Zeier, J. Leker, Battery cost forecasting: a review of methods and results with an outlook to 2050, Energy Environ. Sci. 14 (2021) 4712–4739, https://doi.org/10.1039/D1EE01530C.

[12] J. Figgener, C. Hecht, D. Haberschusz, J. Bors, K.G. Spreuer, K.-P. Kairies, P. Stenzel, D.U. Sauer, The Development of Battery Storage Systems in Germany: A Market Review (Status 2022), 2022, https://doi.org/10.48550/ARXIV.2203.06762.

[13] S. Vögele, W.-R. Poganietz, M. Kleinebrahm, W. Weimer-Jehle, J. Bernhard, W. Kuckshinrichs, A. Weiss, Dissemination of PV-battery systems in the german residential sector up to 2050: technological diffusion from multidisciplinary perspectives, Energy 248 (2022), 123477, https://doi.org/10.1016/j.energy.2022.123477.

[14] K. Mainzer, K. Fath, R. McKenna, J. Stengel, W. Fichtner, F. Schultmann, A high-resolution determination of the technical potential for residential-roof-mounted photovoltaic systems in Germany, Sol. Energy 105 (2014) 715–731, https://doi.org/10.1016/j.solener.2014.04.015.

[15] V. Bertsch, J. Geldermann, T. Lühn, What drives the profitability of household PV investments, self-consumption and self-sufficiency? Appl. Energy 204 (2017) 1–15, https://doi.org/10.1016/j.apenergy.2017.06.055.

[16] Bundesnetzagentur für Elektrizität, Gas, Telekommunikation, Post und Eisenbahnen (BNetzA), Marktstammdatenregister der Bundesnetzagentur, (n.d.). https://www.marktstammdatenregister.de/MaStR (accessed August 3, 2022).

[17] BSW - Bundesverband Solarwirtschaft e.V., Marktdaten: Daten und Infos zur deutschen Solarbranche. https://www.solarwirtschaft.de/presse/marktdaten/, 2022 (accessed July 16, 2022).

[18] D. Fett, C. Fraunholz, D. Keles, Diffusion and system impact of residential battery storage under different regulatory settings, Energy Policy 158 (2021), 112543, https://doi.org/10.1016/j.enpol.2021.112543.

[19] S. Enkhardt, EUPD Research erwartet Installation von 150.000 Photovoltaik-Heimspeichern 2021 – Sonnen und BYD 2020 ganz vorn, Pv Mag. Dtschl. https://www.pv-magazine.de/2021/12/02/sonnen-byd-senec-und-e3-dc-dominieren-weiter-deutschen-markt-fuer-photovoltaik-heimspeicher/, 2021 (accessed July 16, 2022).

[20] S. Enkhardt, Sonnen, BYD, Senec und E3/DC dominieren weiter deutschen Markt für Photovoltaik-Heimspeicher, Pv Mag. Dtschl. https://www.pv-magazine.de/2021/12/02/sonnen-byd-senec-und-e3-dc-dominieren-weiter-deutschen-markt-fuer-photovoltaik-heimspeicher/, 2021 (accessed July 16, 2022).

[21] Pv Magazine, Marktübersicht Batteriespeicher für Photovoltaikanlagen - 2022, Pv Mag. Dtschl. https://www.pv-magazine.de/marktuebersichten/batteriespeicher/produktdatenbank-batteriespeichersysteme-fuer-photovoltaikanlagen/, 2022.

[22] J. Weniger, Bewertung der Energieeffizienz von netzgekoppelten Photovoltaik-Batteriesystemen in Wohngebäuden, Technische Universität Berlin, 2019. Dissertation.

[23] N. Munzke, B. Schwarz, F. Büchle, M. Hiller, Evaluation of the efficiency and resulting electrical and economic losses of photovoltaic home storage systems, J. Energy Storage 33 (2021), 101724, https://doi.org/10.1016/j.est.2020.101724.

[24] J. Weniger, T. Tjaden, J. Bergner, V. Quaschning, Emerging performance issues of photovoltaic battery systems, in: 32nd Eur. Photovolt. Sol. Energy Conf. Exhib., München, 2016, pp. 2372–2380, https://doi.org/10.4229/EUPVSEC20162016-6DP.2.1 (accessed July 26, 2022).

[25] L. Meissner, J. Weniger, N. Orth, V. Quaschning, in: Batteries are getting better, Pv Mag. Int., 2022, pp. 88–90.

[26] DNV GL, Safety, Operation and Performance of Grid-connected Energy Storage Systems, 2017.

[27] 1679-2020, IEEE Recommended Practice for the Characterization and Evaluation of Energy Storage Technologies in Stationary Applications, IEEE, 2020.

[28] M.U. Hassan, S. Saha, M.E. Haque, A framework for the performance evaluation of household rooftop solar battery systems, Int. J. Electr. Power Energy Syst. 125 (2021), 106446, https://doi.org/10.1016/j.ijepes.2020.106446.

[29] S.N. Islam, S. Saha, M.E. Haque, M.A. Mahmud, Comparative analysis of commonly used batteries for residential solar PV applications, in: 2019 IEEE PES Asia-Pac. Power Energy Eng. Conf. APPEEC, IEEE, Macao, Macao, 2019, pp. 1–5, https://doi.org/10.1109/APPEEC45492.2019.8994441.

[30] L. Meissner, J. Weniger, N. Orth, V. Quaschning, Stromspeicher-Inspektion 2021, Hochschule für Technik und Wirtschaft Berlin, Berlin, 2021.

[31] H. Hesse, R. Martins, P. Musilek, M. Naumann, C. Truong, A. Jossen, Economic optimization of component sizing for residential battery storage systems, Energies 10 (2017) 835, https://doi.org/10.3390/en10070835.

[32] N. Munzke, F. Büchle, A. Smith, M. Hiller, Influence of efficiency,aging and charging strategy on the economic viability and dimensioning of photovoltaic home storage systems, Energies 14 (2021) 7673, https://doi.org/10.3390/en14227673.

[33] M. Shabani, E. Dahlquist, F. Wallin, J. Yan, Techno-economic impacts of battery performance models and control strategies on optimal design of a grid-connected PV system, Energy Convers. Manag. 245 (2021), 114617, https://doi.org/10.1016/j.enconman.2021.114617.

[34] N. Orth, J. Weniger, L. Meissner, I. Lawaczeck, V. Quaschning, Stromspeicher-Inspektion 2022, Hochschule für Technik und Wirtschaft Berlin, Berlin, 2022.

[35] J. Moshövel, D. Magnor, D.U. Sauer, S. Gährs, M. Bost, B. Hirschl, M. Cramer, B. Özalay, C. Matrose, C. Müller, A. Schnettler, Analyse des wirtschaftlichen, technischen und ökologischen Nutzens von PV-Speichern, ISEA, 2015.

[36] R.L. Fares, M.E. Webber, The impacts of storing solar energy in the home to reduce reliance on the utility, Nat. Energy 2 (2017), https://doi.org/10.1038/nenergy.2017.1.

[37] Pv Magazine International, Webinar - efficiency is key: the decision criteria for home storage solutions, Pv Mag. Int. https://www.pv-magazine.com/webinars/efficiency-is-key-the-decision-criteria-for-home-storage/, 2021 (accessed July 16, 2022).

[38] K.-P. Kairies, J. Figgener, D. Haberschusz, O. Wessels, B. Tepe, D.U. Sauer, Market and technology development of PV home storage systems in Germany, J. Energy Storage 23 (2019) 416–424, https://doi.org/10.1016/j.est.2019.02.023.

[39] F. Niedermeyer, J. von Appen, A. Schmiegel, N. Kreutzer, A. Reischl, W. Scheuerle, M. Braun, Allgemeine Performanceindikatoren für PV-Speichersysteme, in: 29 Symp. Photovoltaische Solarenergie, Bad Staffelstein, 2014.

[40] J. Thompson, E. Minear, Energy Storage Integration Council (ESIC) Energy Storage Test Manuel, Electric Power Research Institute, Palo Alto, 2021.

[41] H. Hesse, M. Schimpe, D. Kucevic, A. Jossen, Lithium-ion battery storage for the grid—a review of stationary battery storage system design tailored for applications in modern power grids, Energies. 10 (2017) 2107, https://doi.org/10.3390/en10122107.

[42] D. Lubkeman, P. Leufkens, A. Feldman, in: Battery Energy Storage Testing for Grid Standard Compliance and Application Performance, 2011, pp. 1–4.

[43] C. Messner, J. Kathan, C. Seitl, S. Hofmüller, R. Bründlinger, Efficiency and effectiveness of PV battery energy storage systems for residential applications - experience from laboratory tests of commercial products, in: 32nd Eur. Photovolt. Sol. Energy Conf. Exhib., München, 2016, pp. 2381–2392, https://doi.org/10.4229/EUPVSEC20162016-6CO.12.1.

[44] N. Orth, J. Weniger, T. Tjaden, N. Munzke, B. Schwarz, F. Büchle, C. Messner, J. Figgener, D. Haberschusz, V. Quaschning, Vergleich der Energieeffizienz verschiedener PV-Speichersystemkonzepte, in: PV-Symp. 2018, Bad Staffelstein, 2018.

[45] F. Niedermeyer, M. Braun, Comparison of performance-assessment methods for residential PV battery systems, Energies. 13 (2020) 5529, https://doi.org/10.3390/en13215529.

[46] M. Knoop, M. Littwin, MATLAB-basiertes Simulationsmodell zur Berechnung der elektrischen Leistungsflüsse im PV-Speichersystem, in: 32 Symp. Photovoltaische Solarenergie, Bad Staffelstein, 2017.

[47] E. Bamberger, R. Haberl, A. Reber, C. Biba, Heimspeicher-Systemtest: Batteriesysteme auf dem Prüfstand, in: PV-Symp. 2021, Bad Staffelstein, 2021.

[48] A. Piepenbrink, EU efficiency for home storage systems - a new and simple procedure, in: 10th Int. Renew. Energy Storage Conf. IRES 2016, Düsseldorf, 2016.

[49] G. Mulder, H. Popp, W. Kohs, Test Methods for Improved Battery Cell Understanding, 2018.

[50] International Electrotechnical Commission (IEC), IEC 61427-2 - Secondary Cells and Batteries for Renewable Energy Storage General Requirements and Methods of Test - Part 2: On-grid Applications, International Electrotechnical Commission (IEC), France, 2014.

[51] N. Blair, A. Schiek, A. Burrell, M. Keyser, A. Deadman, I. Ellerington, L. Govaerts, G. Mulder, P. Hendrick, T. Polfliet, P. Hannam, C. Song, Global Overview of Energy Storage Performance Test Protocols, 2021, https://doi.org/10.2172/1696786.

[52] D. Conover, A. Crawford, J. Fuller, S. Gourisetti, V. Viswanathan, S. Ferreira, D. Schoenwald, D. Rosewater, Protocol for Uniformly Measuring and Expressing the Performance of Energy Storage Systems, 2016. https://energystorage.pnnl.gov/pdf/PNNL-22010Rev2.pdf.

[53] C. Vartanian, M. Paiss, V. Viswanathan, J. Kolln, D. Reed, Review of codes and standards for energy storage systems, Curr. Sustain. Energy Rep. 8 (2021) 138–148, https://doi.org/10.1007/s40518-021-00182-8.

[54] D. Rosewater, P. Scott, S. Santoso, Application of a uniform testing protocol for energy storage systems, in: 2017 IEEE Power Energy Soc. Gen. Meet, IEEE, Chicago, IL, 2017, pp. 1–5, https://doi.org/10.1109/PESGM.2017.8274603.

[55] A.J. Crawford, V.V. Viswanathan, C.K. Vartanian, M.J.E. Alam, P.J. Balducci, D. Wu, T.D. Hardy, K. Mongird, Avista Turner Energy Storage System: Assessment of Battery Technical Performance, 2019, https://doi.org/10.2172/1557266.

[56] D. Rosewater, S. Ferreira, Development of a frequency regulation duty-cycle for standardized energy storage performance testing, J. Energy Storage 7 (2016) 286–294, https://doi.org/10.1016/j.est.2016.04.004.

[57] D.M. Davies, M.G. Verde, O. Mnyshenko, Y.R. Chen, R. Rajeev, Y.S. Meng, G. Elliott, Combined economic and technological evaluation of battery energy storage for grid applications, Nat. Energy 4 (2019) 42–50, https://doi.org/10.1038/s41560-018-0290-1.

[58] National Electrical Manufactures Association (NEMA), Standard for Uniformly Measuring and Expressing the Performance of Electrical Energy Storage Systems, National Electrical Manufactures Association (NEMA), Rosslyn, 2019.

[59] International Electrotechnical Commission (IEC), IEC 62933-2-1 - Electrical Energy Storage (EES) Systems–Part 2-1: Unit Parameters and Testing Methods–General Specification, International Electrotechnical Commission (IEC), Geneva, 2017.

[60] International Electrotechnical Commission (IEC), IEC 62933-2-2 - Electrical Energy Storage (EES) Systems–Part 2-2: Unit Parameters and Testing Methods–Application and Performance Testing, International Electrotechnical Commission (IEC), Geneva, 2022.

[61] International Electrotechnical Commission (IEC), IEC 62933-3-1 - Electrical Energy Storage (EES) Systems–Part 3-1: Planning and Performance Assessment of Electrical Energy Storage Systems – General Specification, International Electrotechnical Commission (IEC), Geneva, 2018.

[62] A. Barai, K. Uddin, M. Dubarry, L. Somerville, A. McGordon, P. Jennings, I. Bloom, A comparison of methodologies for the non-invasive characterisation of commercial Li-ion cells, Prog. Energy Combust. Sci. 72 (2019) 1–31, https://doi.org/10.1016/j.pecs.2019.01.001.

[63] S.S. Kulkarni, F. Büchle, N. Munzke, W. Heckmann, N. Giesen, C. Messner, Effizienzleitfaden für PV-Speichersysteme - Wiederholbarkeit und Einfluss von Mess- und Auswerteparametern, 2022, https://doi.org/10.13140/RG.2.2.30164.27526.

[64] D. Choi, N. Shamim, A. Crawford, Q. Huang, C.K. Vartanian, V.V. Viswanathan, M.D. Paiss, M.J.E. Alam, D.M. Reed, V.L. Sprenkle, Li-ion battery technology for grid application, J. Power Sources 511 (2021), 230419, https://doi.org/10.1016/j.jpowsour.2021.230419.

[65] International Electrotechnical Commission (IEC), IEC 61683 - Photovoltaic systems – Power conditioners – Procedure for measuring efficiency, International Electrotechnical Commission (IEC), Geneva, 1999.

[66] CENELEC members, European Standard EN 50530:2010 - Overall Efficiency of Grid Connected Photovoltaic Inverters, Brussels, Belgium, 2010.

[67] ITP Renewables, Lithium Ion Battery Testing - Public Report 12 (Final Report), ITP Renewables, Canberra, Australien, 2022. https://batterytestcentre.com.au.

[68] C. Messner, J. Kathan, J. Mayr, Effizienz und Effektivität von netzgekoppelten PV-Heimspeichersystemen - Erfahrungen und Erkenntnisse aus Labortests kommerzieller Produkte, in: 31 Symp. Photovoltaische Solarenergie, Bad Staffelstein, 2016.

[69] M. Munzke, B. James, B. Schwarz, Performance evaluation of household Li-ion battery storage systems, in: 32nd Eur. Photovolt. Sol. Energy Conf. Exhib., München, 2016, pp. 1516–1521, https://doi.org/10.4229/EUPVSEC20162016-5AO.9.5.

[70] F. Niedermeyer, J. von Appen, T. Kneiske, M. Braun, A. Schmiegel, N. Kreutzer, M. Rothert, A. Reischl, Innovative Performancetests für PV-Speichersysteme zur Erhöhung der Autarkie und des Eigenverbrauchs, in: 30 Symp. Photovoltaische Solarenergie, Bad Staffelstein, 2015.

[71] K.-P. Kairies, D. Haberschusz, J. van Ouwerkerk, J. Strebel, O. Wessels, D. Magnor, J. Badeda, D.U. Sauer, Wissenschaftliches Mess- und Evaluierungsprogramm Solarstromspeicher - Jahresbericht 2016, Institut für Stromrichtertechnik und Elektronische Antriebe (ISEA), RWTH Aachen, Aachen, 2016.

[72] Bundesverband Energiespeicher e.V. (BVES), Bundesverband Solarwirtschaft (BSW), Efficiency guideline for PV storage systems 2.0, Berlin. https://www.bves.de/effizienzleitfaden_3_2019/, 2019.

[73] G.B.M.A. Litjens, E. Worrell, W.G.J.H.M. van Sark, Assessment of forecasting methods on performance of photovoltaic-battery systems, Appl. Energy 221 (2018) 358–373, https://doi.org/10.1016/j.apenergy.2018.03.154.

[74] F. Büchle, N. Munzke, B. Schwarz, M. Hiller, C. Messner, S. Lux, J.Klee Barillas, Lithium-Ionen Heimspeichersysteme: Reproduzierbarkeit von Performancemessungen an PV-Speichersystemen, in: PV-Symp. 2018, Bad Staffelstein, 2018.

[75] N. Munzke, M. Mast, B. Schwarz, F. Büchle, L. Beeh, S. Lux, N. Kevlishvili, B. Mademann, J.Klee Barillas, H. Döring, Safety First – Sichere netzdienliche Heimspeicher, 2019 (accessed July 16, 2022).

[76] N. Munzke, B. Schwarz, F. Büchle, J. Barry, Lithium-Ionen Heimspeichersysteme: Performance auf dem Prüfstand, in: 32 Symp. Photovoltaische Solarenergie, Bad Staffelstein, 2017.

[77] N. Munzke, B. Schwarz, M. Hiller, Intelligent control of household Li-ion battery storage systems, Energy Procedia 155 (2018) 17–31, https://doi.org/10.1016/j.egypro.2018.11.069.

[78] F. Niedermeyer, Performance Assessment of Residential PV Battery Systems: Development and Application of Test Procedures and Key Performance Indicators, Universität Kassel, 2021.

[79] J. Weniger, S. Maier, L. Kranz, N. Orth, N. Böhme, V. Quaschning, Stromspeicher-Inspektion 2018, Hochschule für Technik und Wirtschaft Berlin, Berlin, 2018.

[80] J. Weniger, N. Orth, N. Böhme, V. Quaschning, Stromspeicher-Inspektion 2019, Hochschule für Technik und Wirtschaft Berlin, Berlin, 2019.

[81] J. Weniger, S. Maier, N. Orth, V. Quaschning, Stromspeicher-Inspektion 2020, Hochschule für Technik und Wirtschaft Berlin, Berlin, 2020.

[82] J. Weniger, T. Tjaden, J. Bergner, V. Quaschning, Sizing of battery converters for residential PV storage systems: how much rated power is sufficient?, in: 10th Int. Renew. Energy Storage Conf. Exhib. IRES 2016, Düsseldorf, 2016.

[83] B. Boeckl, T. Kienberger, Sizing of PV storage systems for different household types, J. Energy Storage 24 (2019), 100763, https://doi.org/10.1016/j.est.2019.100763.

[84] J. Figgener, P. Stenzel, K.-P. Kairies, J. Linßen, D. Haberschusz, O. Wessels, M. Robinius, D. Stolten, D.U. Sauer, The development of stationary battery storage systems in Germany – status 2020, J. Energy Storage 33 (2021), 101982, https://doi.org/10.1016/j.est.2020.101982.

[85] J. Li, M.A. Danzer, Optimal charge control strategies for stationary photovoltaic battery systems, J. Power Sources 258 (2014) 365–373, https://doi.org/10.1016/j.jpowsour.2014.02.066.

[86] G. Angenendt, S. Zurmühlen, H. Axelsen, D.U. Sauer, Comparison of different operation strategies for PV battery home storage systems including forecast-based operation strategies, Appl. Energy 229 (2018) 884–899, https://doi.org/10.1016/j.apenergy.2018.08.058.

[87] P. Keil, S.F. Schuster, J. Wilhelm, J. Travi, A. Hauser, R.C. Karl, A. Jossen, Calendar aging of lithium-ion batteries, J. Electrochem. Soc. 163 (2016) A1872–A1880, https://doi.org/10.1149/2.0411609jes.

[88] M. Schimpe, M. Naumann, N. Truong, H. Hesse, S. Santhanagopalan, A. Saxon, A. Jossen, Energy efficiency evaluation of a stationary lithium-ion battery container storage system via electro-thermal modeling and detailed component analysis, Appl. Energy (2018) 211–229.

[89] V. Vega-Garita, L. Ramirez-Elizondo, G.R.C. Mouli, P. Bauer, Review of residential PV-storage architectures, in: Energy Conf. ENERGYCON 2016 IEEE Int., Leuven, 2016, pp. 1–6, https://doi.org/10.1109/ENERGYCON.2016.7514039.

[90] P.J. Rechberger, G. Steinmaurer, R. Reder, Control algorithms for photovoltaic inverters with battery storage for increased self consumption, in: Proc. Int. Workshop Simul. Energy Sustain. Dev. Environ. SESDE, Athen, 2013. http://www.asic.at/fileadmin/user_upload/Media/PDFs/Rechberger_Paper_Control_Algorithms_final.pdf.

[91] F.P. Baumgartner, H. Schmidt, B. Burger, R. Bründlinger, H. Häberlin, M. Zehner, Status and relevance of the DC voltage dependency of the inverter efficiency, in: 22nd Eur. Photovolt. Sol. Energy Conf. Exhib., Milan, 2007 (accessed July 26, 2022).

[92] F. Kever, in: Unterschiedliche Schaltungen, unterschiedliche Effizienzen, Pv Mag, 2013, pp. 109–112.

[93] W.-T. Franke, Neues Schaltungskonzept zur Energiespeicherung bei Solarwechselrichtern, in: 27 Symp. Photovoltaische Solarenergie, Bad Staffelstein, 2012.

[94] M. Rothert, A.S. Bukvic-Schäfer, T. Thierschmidt, Performance von Speichersystemen in der Praxis - Erfahrungen von über 6.500 Speichersystemen, 2015. Niestetal.

[95] G. Angenendt, B. Ashrafinia, S. Zurmühlen, K. Jacqué, J. Badeda, D.-U. Sauer, Influence of the battery voltage level on the efficiency and cost of a PV battery energy storage system, in: 32 Symp. Photovoltaische Solarenergie, Bad Staffelstein, 2017.

[96] D.U. Sauer, Untersuchungen zum Einsatz und Entwicklung von Simulationsmodellen für die Auslegung von Photovoltaik-Systemen, Diplomarbeit, Technische Hochschule Darmstadt, 1994.

[97] M. Braun, K. Büdenbender, D. Magnor, A. Jossen, Photovoltaic self-consumption in Germany - using lithium-ion storage to increase self-consumed photovoltaic energy, in: 24th Eur. Photovolt. Sol. Energy Conf., Hamburg, 2009, pp. 3121–3127, https://doi.org/10.4229/24thEUPVSEC2009-4BO.11.2.

[98] L. Probst, D. von Kutzleben, C. Armbruster, C. Schöner, Partial-load optimization of a high-voltage residential battery converter with silicon carbide MOSFETs, in: PCIM Eur. 2019, Nürnberg, 2019.

[99] K.-P. Kairies, D. Haberschusz, O. Wessels, J. Strebel, J. van Ouwerkerk, D. Magnor, D.U. Sauer, Real-life load profiles of PV battery systems from field measurements, Energy Procedia 99 (2016) 401–410, https://doi.org/10.1016/j.egypro.2016.10.130.

[100] Pv Magazine Deutschland, Webinar - Die neue Stromspeicherinspektion 2020 ist erschienen: Was bedeuten die Ergebnisse für Installateure und Kunden?, Pv Mag. Dtschl. https://www.pv-magazine.de/webinare/die-neue-stromspeicherinspektion-2020-ist-erschienen-was-bedeuten-die-ergebnisse-fuer-installateure-und-kunden/, 2020 (accessed June 25, 2022).

[101] M. Graff, O. Wollersheim, J. May, Towards reproducible performance of grid connected photovoltaic battery storage, in: 15th Int. Conf. Renew. Energy Storage IRES, Online, 2021.

[102] J. Weniger, T. Tjaden, J. Bergner, V. Quaschning, Dynamic mismatch losses of grid-connected PV-battery systems in residential buildings, J. Energy Storage 13 (2017) 244–254, https://doi.org/10.1016/j.est.2017.07.011.

[103] K. Lappalainen, S. Valkealahti, Recognition and modelling of irradiance transitions caused by moving clouds, Sol. Energy 112 (2015) 55–67, https://doi.org/10.1016/j.solener.2014.11.018.

[104] M. Hayn, V. Bertsch, W. Fichtner, Electricity load profiles in Europe: the importance of household segmentation, Energy Res.Soc. Sci. 3 (2014) 30–45, https://doi.org/10.1016/j.erss.2014.07.002.

[105] S. Cao, K. Sirén, Impact of simulation time-resolution on the matching of PV production and household electric demand, Appl. Energy 128 (2014) 192–208, https://doi.org/10.1016/j.apenergy.2014.04.075.

[106] J. Pinne, Optimierung von PV-Wechselrichtern im Netzparallelbetrieb mithilfe analytischer Verhaltens- und Verlustleistungsmodelle, Kassel University Press, Kassel, 2015.

[107] C. Messner, Performance Evaluation of Grid-connected PV Battery Energy Storage Systems for Residential Applications, TU Wien, 2016. Masterthesis.

[108] T. Grün, K. Stella, O. Wollersheim, Influence of circuit design on load distribution and performance of parallel-connected lithium ion cells for photovoltaic home storage systems, J. Energy Storage 17 (2018) 367–382, https://doi.org/10.1016/j.est.2018.03.010.

[109] F. Ackermann, T. Bülo, C. Nöding, Untersuchungen von Einflussgrößen auf Wirkungsgrad- und Leistungsmessungen von PV-Wechselrichtern, in: 26 Symp. Photovoltaische Solarenergie, Bad Staffelstein, 2011.

[110] J. Despeghel, J. Tant, J. Driesen, Loss model for improved efficiency characterization of DC coupled PV-battery system converters, in: IECON 2019 - 45th Annu. Conf. IEEE Ind. Electron. Soc., Lisbon, 2019, p. 6, https://doi.org/10.1109/IECON.2019.8927644.

[111] H. S, Overview of cell balancing methods for Li-ion battery technology, Energy Storage 3 (2021), https://doi.org/10.1002/est2.203.

[112] A. Vezzini, Lithium-ion battery management, in: Lithium-Ion Batter, Elsevier, 2014, pp. 345–360, https://doi.org/10.1016/B978-0-444-59513-3.00015-7.

[113] SMA Solar Technology AG, eMANUAL: SUNNY ISLAND 4.4M/6.0H/8.0H. https://manuals.sma.de/SI-13/de-DE/index.html, 2022 (accessed July 28, 2022).

[114] LG, LG Installation Manuel: Residential Battery Unit, 2022.

[115] J. Moshövel, K.-P. Kairies, D. Magnor, M. Leuthold, M. Bost, S. Gährs, E. Szczechowicz, M. Cramer, D.U. Sauer, Analysis of the maximal possible grid relief from PV-peak-power impacts by using storage systems for increased self-consumption, Appl. Energy 137 (2015) 567–575, https://doi.org/10.1016/j.apenergy.2014.07.021.

[116] G. Angenendt, S. Zurmühlen, R. Mir-Montazeri, D. Magnor, D.U. Sauer, Enhancing battery lifetime in PV battery home storage systems using forecast based operating strategies, in: 10th Int. Renew. Energy Storage Conf. IRES 2016, Düsseldorf, 2016. Masterthesis.

[117] A.U. Schmiegel, A. Linhart, C. Jehoulet, H. Schuh, M. Landau, M. Braun, K. Büdenbender, D.U. Sauer, D. Magnor, J. Binder, H.D. Mohring, The sol-ion system: realizing safety and efficiency for a PV storage system, in: 26th Eur. Photovolt. Sol. Energy Conf. Exhib., Hamburg, 2011, https://doi.org/10.4229/26theupvsec2011-5bv.1.34.